TALLINN UNIVERSITY OF TECHNOLOGY
Faculty of Information Technology

IE70LT

Denry Aron 153757IVEM

DUAL OUTPUT, UNIVERSAL INPUT OFF-LINE POWER SUPPLY

Master's thesis

Supervisor: Juri Mihhailov
PhD
Visiting Lecturer

Tallinn 2017

TALLINNA TEHNIKAÜLIKOOL
Infotehnoloogia teaduskond

IE70LT

Denry Aron 153757IVEM

KAHE VÄLJUNDIGA, UNIVERSAALSE VAHEMIKUGA VÕRGUSISENDIGA TOITESEADE

Magistritöö

Juhendaja: Juri Mihhailov
Doktorikraad
Külalislektor

Tallinn 2017

Author’s declaration of originality

I hereby certify that I am the sole author of this thesis. All the used materials, references to the literature and the work of others have been referred to. This thesis has not been presented for examination anywhere else.

Author: Denry Aron

05.05.2017

Abstract

Given thesis describes a power converter, which performs conversion from mains network to low-voltage outputs.The thesis describes converter controller, transformer design, performance, safety aspects and PCB of the device. The device described here is intended to be integrated into specific product.

Process described here consisted of schematic design, including choice of components and PCB design.

This thesis is written in English and is 78 pages long, including 14 chapters, 38 illustrations and 16 tables.

Annotatsioon

Kahe väljundiga, universaalvahemikuga võrgusisendiga toiteseade

Antud lõputöö kirjeldab toitemuundurit, mille eesmärgiks on võrgupingest luua madalapingelised väljundid. Lõputöö kirjeldab muunduri juhtseadet, transformaatori väljatöötust, jõudlust, ohutusaspekte ning trükkplaadi küljendamist. Kirjeldatud seade on ette nähtud integreerimiseks kindlasse tootesse.

Siin kirjeldatud protsess sisaldab skeemi väljatöötlust, sealhulgas komponentide valikut ning trükkplaadi küljendamist.

Lõputöö on kirjutatud inglise keeles ning sisaldab teksti 78 leheküljel, 14 peatükki, 38 joonist, 16 tabelit.

List of abbreviations and terms

BOM	Bill of materials
EA	Error amplifier
ELV	Extra-low voltage
EMI	Electromagnetic inteference
IC	Integrated circuit
ITE	Information technology equipment
LED	Light emitting diode
LISN	Line Impedance Stabilization Network
PCB	Printed circuit board
PE	Protective earth
PF	Power factor
PMIC	Power management integrated circuit
RMS	Root mean square
SMD	Surface-mount device
TI	Texas Instruments
TVS	Transient-voltage surpressor

Table of Contents

1 Background for topic......12
2 State-of-the-art research......13
2.1 Options......13
2.1.1 Mains frequency transformer......13
2.1.2 Linear regulator......14
2.1.3 Switching, forward converter......15
2.1.4 Switching, double-ended forward converter......16
2.1.5 Switching, interleaved forward converter......17
2.1.6 Switching, buck converter......18
2.1.7 Switching, flyback......19
2.1.8 Switching, push-pull......20
3 Conclusion of research......21
4 Further research of optimal options......22
4.1 Switching element......22
4.2 Feedback source......22
5 Feasibility study......23
5.1 Cost......23
5.2 Time to market......24
5.3 Size (integration)......25
6 Selection of controller......26
6.1 Operation principle of controller......27
7 Calculation of transformer......29
7.1 Choice of bobbin and core......29
7.2 Calculation of windings......31
8 Snubber......40
9 Filtering......42
9.1 Common mode......42
9.2 Differential mode......43
10 Power factor correction......44

11 Initial prototype......45
11.1 Various tests......51
11.2 Lessons learned......57
12 Second prototype......59
12.1 Various tests......62
12.1.1 Efficiency......62
12.1.2 Ferrite types......64
12.2 Noise......64
12.2.1 Output noise......64
12.3 Power factor......67
12.4 Inrush......68
12.5 Undervoltage and overvoltage......69
12.6 Operation temperature......69
13 Safety aspects......71
13.1 Creepages and clearances......71
14 Summary......74
Sources......75
Appendix 1 - BOM for first prototype......77
Appendix 2 - BOM for second prototype......78

List of Figures

Figure 1. Mains frequency transformer topology......13
Figure 2. Linear regulator topology......14
Figure 3. Forward converter topology......15
Figure 4. Double-ended forward converter topology......16
Figure 5. Topology of interleaved forward converter......17
Figure 6. Topology of buck converter......18
Figure 7. Flyback converter topology......19
Figure 8. Push-pull converter topology......20
Figure 9. Drain waveform in quasi-resonant mode[6]......27
Figure 10. Example waveforms of feedback in quasi-resonant controller [8]......28
Figure 11. Gap to AL factor from N87 E20 datasheet......30
Figure 12. Core gap in relation to AL value......31
Figure 13. Example of multiple intertwined parallels from a testing transformer......39
Figure 14. RCD snubber example......40
Figure 15. Filtering layout......42
Figure 16. Common-mode choke frequency characteristic......43
Figure 17. Example of non-unity power factor......44
Figure 18. Schematic of initial prototype......45
Figure 19. C3225X7S1H106K250AB DC bias graph......46
Figure 20. TMK212BBJ106KGHT DC bias graph......47
Figure 21: First prototype with operation loops highlighted......50
Figure 22. First prototype with snubber loops highlighted......50
Figure 23. Failing quasi-resonant behaviour......52
Figure 24. Controller waveform on a working example board......53
Figure 25. 2000 µH inductance in primary......54
Figure 26. Waveforms after increasing primary inductance......55
Figure 27. Waveforms while controller loops starting......56
Figure 28. Same as figure 27, but zoomed......56
Figure 29. Voltage control principle: internal schematic, for Altair05T......57

Figure 30. Schematic of second prototype....59
Figure 31. Efficiency results....63
Figure 32. Efficiency of reference design....63
Figure 33. Output ripples at 115 VAC input voltage....65
Figure 34. Output ripples at 230 VAC input voltage....66
Figure 35. Input voltage and current waveform - 115 VAC....68
Figure 36. Input voltage and current waveform - 230 VAC....68
Figure 37. Inrush measurement....69
Figure 38. Creepage and clearance visualised....71

List of Tables

Table 1. Power supply bill of materials estimate (primary cost drivers)........................24
Table 2. Drain-to-Source voltage parameter comparison...26
Table 3. Ferrite material comparison...30
Table 4. Initial transformer input values...32
Table 5. Thicknesses of wires for windings..38
Table 6. Transformer windings details..38
Table 7. Output diode VSDRRM requirements...49
Table 8. Primary inductance values...54
Table 9. Transformer windings for higher inductance...55
Table 10. Maximum output power...62
Table 11. Efficiency results...63
Table 12. Maximum load with various core materials..64
Table 13. Power factor results...67
Table 14. Temperature measurement results...70
Table 15. Power supply voltage map...72
Table 16. Outer layer creepages, in mm...73

1 Background for topic

The power supply, development of which is addressed in this paper, is designed with the goal to be integrated into another product. Primary use case for outputs is powering 12 VDC relays and 3.3 VDC circuitry (microcontroller, radios etc).

As estimated quantities were large enough (thousands per year), it was necessary to look into reducing cost per unit, e.g. comparing power supplies available as modules and designing one from ground up.

Another justifying factor for looking into custom power supply is the integration - it can be more efficient and also aesthetically pleasing to combine logic and power circuitry on a single PCB.

2 State-of-the-art research

As the estimated power requirement is within the range of 10-20 watts, this is taken into account while developing. Initial specification for design is 1.0 A at 4 VDC for main output and 0.4 A at 12 VDC for additional output. Universal input (115/230 VAC, 50/60 Hz). For user safety, power supply output must be isolated from mains.

For final product, cost of production needs to be minimal, however optimal tradeoff for price and quality is necessary to be found.

2.1 Options

Various topologies, their positive and negative features and through that their suitability shall be analyzed.

2.1.1 Mains frequency transformer

This option consists of a transformer, capable of outputting the required 10-20 VA at specified voltages, rectifier, capacitor and optional additional smoothing (e.g. L-C-L filter) [1].

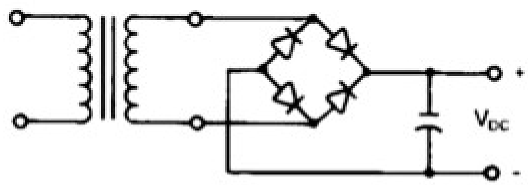

Figure 1. Mains frequency transformer topology.

Pros:

- Simple
- Robust
- Galvanic isolation

Cons:

- 115/230 VAC switching requires user input (possible hazard) or additional circuitry

- Price (for higher powers remarkable material cost) (6.95 USD for 20 VA transformer at quantity of 10,000, source: Digi-Key)
- Heavy (more windings for mains frequency)
- Output varying as a function of load, requires additional circuitry for stabilisation

This design is not too innovative, however most likely to work. The input and output voltage relation is directly in relation with transformer turns.

$$\frac{Turns_{primary}}{Turns_{secondary}} = \frac{V_{primary}}{V_{secondary}} \tag{1}$$

2.1.2 Linear regulator

Component in series between input and output, adjusting internal resistance according to output voltage deviation to keep it as close to target value as possible [2].

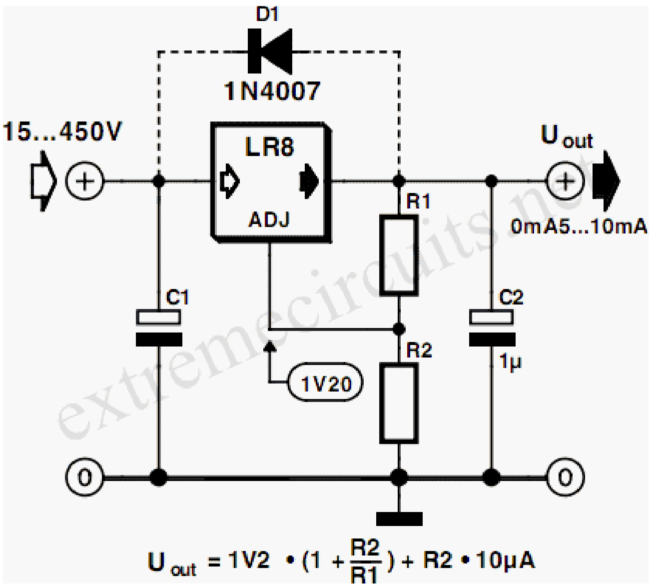

Figure 2. Linear regulator topology.

Pros:

- Simple
- Fairly precise and stable output voltage
- No transformer

- Lightweight (excluding heatsink)

Cons:

- Remarkable losses (for initially specified output, roughly 444.8 W of wasted power)
- Hard to find models capable of withstanding ~324 VDC (rectified 230 VAC RMS) input voltage (unless using discrete components)
- Output not isolated from mains power supply

For this application this is not suitable, however for minimal current output it might be a reasonable solution. Finding output voltage for this type is dependent on the load.

$$V_{out} = I_{out} \cdot R_{load} \tag{2}$$

2.1.3 Switching, forward converter

This topology takes DC input and adds oscillation to drive the transformer. Frequency used it higher than typical mains network, allowing for smaller transformer [3].

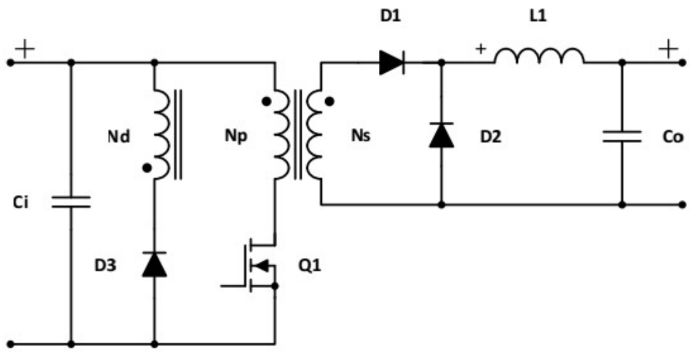

Figure 3. Forward converter topology.

Pros:

- Galvanic isolation

Cons:

- Transistor experiences stress of 2x Vin
- Aside from primary, return winding also necessary

- Output inductors (with freewheeling diodes) essential

As with most switching converters, this requires feedback to primary for adjusting output voltage via duty cycle (switching element on-time).

$$V_{secondary} = \frac{(Duty\,cycle) \cdot Turns_{secondary} \cdot V_{in}}{Turns_{primary}} \quad (3)$$

2.1.4 Switching, double-ended forward converter

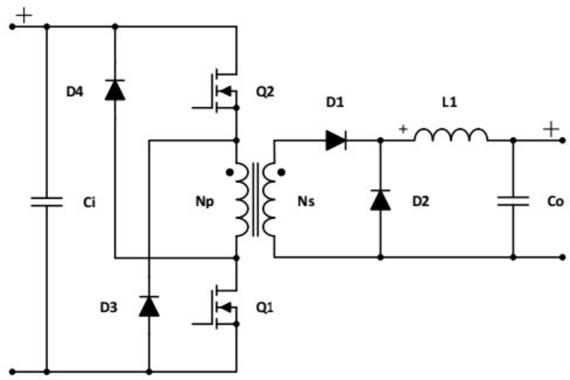

Figure 4. Double-ended forward converter topology.

Forward converter with an additional switching element [3].

Pros:

- Reduces voltage spike on transistor (1x Vin per transistor)
- Single primary winding
- Galvanic isolation

Cons:

- Two transistors
- Output inductors (with freewheeling diodes) essential

Output voltage formula is identical to single-ended forward converter.

2.1.5 Switching, interleaved forward converter

This topology consists of two forward converters running in parallel [4].

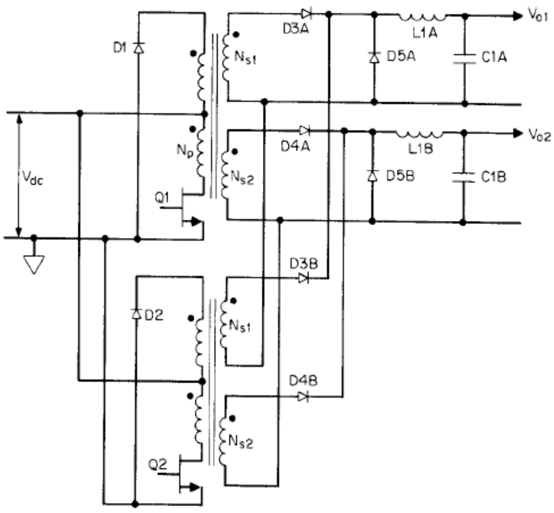

Figure 5. Topology of interleaved forward converter.

Pros:

- Reduced load on transistor
- Galvanic isolation
- Less EMI

Cons:

- Double transformer size compared to forward converter
- Double amount of transistors and rectifying elements than forward converter
- Two signals for switching (note: dead-time not critical)
- Output inductors (with freewheeling diodes) essential

Output voltage formula is identical to single-ended forward converter.

2.1.6 Switching, buck converter

This topology switches input power to output at high frequency with variable duty cycle, which after filtering results in a percentage of input voltage [3].

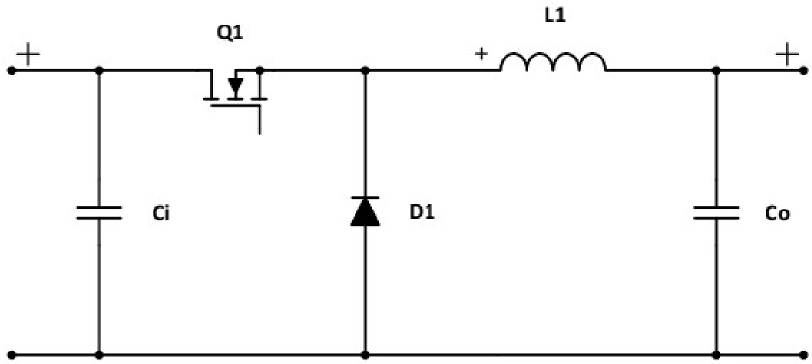

Figure 6. Topology of buck converter.

Pros:

- No transformer
- Low weight

Cons:

- Output not isolated from mains power supply
- Single output

$$V_{out} = (Duty\ cycle) \cdot V_{in} \tag{4}$$

2.1.7 Switching, flyback

Flyback uses transformer with primary winding inverted, transferring power from transformer to output while the primary switch is not conducting [3].

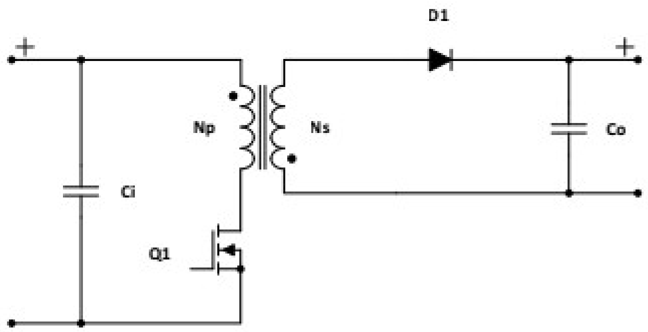

Figure 7. Flyback converter topology.

Pros:

- Galvanic isolation
- Output inductors not necessary to filter switching noise
- Output voltages (for multiple output) compensate each other
- Of topologies considered, most likely to perform safely and reliably with universal input
- Small footprint

Cons:

- Snubber/clamp circuit necessary
- Most significant risk for creating EMI

The output voltage calculation is dependent on the load, as the transfer ratio is based on current not voltage, and regulated through duty cycle.

This is further explained in chapter 7 Calculation of transformer.

2.1.8 Switching, push-pull

Push-pull topology alternates the current directory in transformer primary, removing the power transfer idle time which is typically covered with freewheeling diode [3].

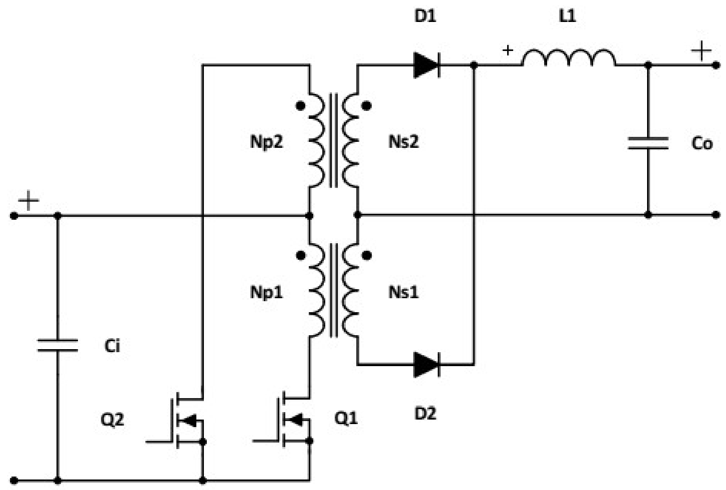

Figure 8. Push-pull converter topology.

Pros:

- No losses from freewheeling diode, emulating mains frequency transformer action
- Load divided between two transistors
- Galvanic isolation

Cons:

- Unbalanced load on primary windings may cause unexpected saturation ("staircase saturation")
- Bigger than forward converter (in cost and size)
- Higher core losses (greater flux excursion)
- Two signals for switching (note: dead-time not critical)
- More rectifying elements in secondary
- Double the amount of primary and secondary windings
- Output inductors (with freewheeling diodes) essential

3 Conclusion of research

After removing topologies that do not offer the required galvanic isolation, we are left with an option to choose one of the designs featuring a transformer. For optimal price and size, one of the switching topologies should be chosen, as output from mains frequency transformer would need additional stabilising circuitry.

As the target is to have multiple outputs and low-cost, flyback converter seems to be the most reasonable choice. This is due to the multiple outputs tracking each other's voltage and current-based transfer which is beneficial when wide input voltage range is necessary.

4 Further research of optimal options

As the era when building devices out of discrete components was reasonable has passed, next step is to browse available Power Management Integrated Circuits (PMICs) and choose a suitable device. This allows us to keep footprint (and due to component count also cost) to minimal.

4.1 Switching element

As an extra component is likely to add price to component (both, for single component price and in assembly process), integrated switching element may be a reasonable choice. Due to power requirement remaining under 20 watts, multiple options with integrated switching element are available, e.g. STMicroelectronics' VIPER22AS-E (suitable for up to 12 watt output power with universal input). As the requirement is 8.8 watt, this is a suitable example.

4.2 Feedback source

As the output load is not fixed, feedback from output is necessary to operate in constant voltage mode. Various PMICs rely on the feature of flyback topology, which causes windings to follow each other's output voltages. This means the output voltage is sensed via a separate winding, allowing the optocoupler (for isolated feedback) and voltage reference to be omitted. This is likely to reduce cost of production even further. (͡° ͜ʖ ͡°)

This may require a performance evaluation prior to making a decision or alternatively a PMIC which is suitable for both feedback options should be chosen to reduce risks during development/prototyping.

5 Feasibility study

Project's feasibility is considered from the following aspects:

1) Cost
2) Time to market
3) Size (integration)

Feasibility is viewed as "is it reasonable", as compared to "is it possible". Considering that similar products are available on the market defeats the purpose of asking the latter question.

5.1 Cost

One should expect to find fairly equivalent power supplies at prices starting from 25€ [5]. Even at high quantities (e.g. 1,000 pieces or more) the cost does not drop below 20€ per unit. As for the output voltage, the example given had fairly similar rating to the required output of the device in question. Assuming less common outputs are necessary, the cost can rise further.

To compare the feasibility from cost perspective, it is necessary to analyze the primary components and their price.

Table 1. Power supply bill of materials estimate (primary cost drivers).

Component	**Quantity per unit**	**Example part**	**Price in eur (quantity of 1000)**	**Notes**
Controller	1	VIPER26HD (STMicroelectronics)	0.68	http://ee.farnell.com/stmicroelectronics/viper26hd/ac-dc-conv-flyback-nsoic-16/dp/2612164
Transformer	1	750311771 (Wurth Electronics)	4.86	http://www.digikey.com/product-detail/en/wurth-electronics-midcom/750311771/732-2667-2-ND/2445674
Input rectifier	1	MDB6S (ON Semiconductor)	0.1	http://www.digikey.com/product-detail/en/fairchild-on-semiconductor/MDB6S/MDB6SFSCT-ND/3137112
Input capacitors	1	EEU-ED2W220S (Panasonic-Electronic-components)	1.42	http://www.digikey.com/product-detail/en/panasonic-electronic-components/EEU-ED2W220S/P13560-ND/1086785
Output capacitors	2	UBT1H471MHD1TO (Nichicon)	0.55	http://www.digikey.com/product-detail/en/nichicon/UBT1H471MHD1TO/493-4510-3-ND/2649098
Output rectifier	2	SK310A-LTP (Micro Commercial Co)	0.11	http://www.digikey.com/product-detail/en/micro-commercial-co/SK310A-LTP/SK310A-LTPMSCT-ND/2642066
Filtering (common-mode choke)	1	744862250 (Wurth-electronics-inc)	2.68	http://www.digikey.com/product-detail/en/wurth-electronics-inc/744862250/732-3145-5-ND/2626083
Filtering (X2 capacitors)	2	ECQ-U2A104ML (Panasonic-electronic-components)	0.09	http://www.digikey.com/product-detail/en/panasonic-electronic-components/ECQ-U2A104ML/P10730-ND/281393
Circuit protection	1	RST 500 AMMO (Bel Fuse Inc)	0.15	http://www.digikey.com/product-detail/en/bel-fuse-inc/RST-500-AMMO/507-1722-3-ND/814043
SUM			**11.39**	

Although this table is fairly simplified, it should give a rough estimate what is the expected cost for bill of materials. It should be noted that the PCB of the product is not in the table, as it will be necessary nevertheless assuming the power supply is part of the same board as the powered device.

Comparing 11-12€ of power supply bill of materials and 20-30€ pre-made supply justifies the development of integrated power supply.

5.2 Time to market

As the development time can be significant, this may be the biggest pitfall for feasibility. This can be justified by the fact, that after the development of first power supply, it is likely to be modified fairly easily for future products. This can be as easy as change of transformer and/or change of component values in feedback circuitry.

Additionally, an off-line power supply can be considered a separate module of the end-product. Therefore development can be spread out in multiple branches, where one engineer is designing the power supply while the other is working on logic circuitry. For the second engineer it is likely to be fairly similar task as if the power supply was chosen as pre-made.

One cause for increase in development time may be the integration of both devices. Assuming a section of PCB is designated for power supply, this potential risk is reduced to minimal.

5.3 Size (integration)

Commercial power supply units typically come with rectangular PCB, size of which is not necessarily standardised. Depending on the PCB size of the device being powered, they may not fit together very well (e.g. one is long and thin, whereas the other one is wide). This creates additional work for mechanical engineers, who are responsible for creating enclosure for the device.

Integration of power supply on the device's PCB allows any shape of board. It is likely that even a hole in the board is allowed, should the application require it.

Another feature of integration appears in the final stages of manufacturing. As electronics devices often include hand-assembly for fixing PCBAs into enclosures, less parts are necessary to mount (one board instead of two), allowing for faster assembly. This results in slightly lower manufacturing cost. Lowering the costs further is the lack of need for special cabling, connecting power supply and consumer.

6 Selection of controller

As discussed in state of the art research, one of the aspects considered while selecting the controller is integrated switch. This has benefits such as:

Reduced cost in manufacturing (SMD assembly cost per detail)

Smaller footprint (sum of multiple casings is larger than single)

Integrated driver for switching element

This criteria leaves fairly wide selection of controllers, therefore more specific choice was made based on switching element drain-to-source voltage rating. The choice is based on this parameter as this indicates how much abuse can the controller take. In turn, providing better reliability. The controller chosen, Altair05T-800, has fairly high rating for this parameter. For reference some alternatives are put into comparison:

Table 2. Drain-to-Source voltage parameter comparison.

Model	Manufacturer	Vds rating
Altair05T-800	STMicroelectronics	800
VIPER12	STMicroelectronics	730
UCC28881	Texas Instruments	700
ICE3B0365J-T	Infineon	650

Additionally, chosen controller differs from typical flyback controllers in two aspects:

- it acquires feedback from auxiliary winding, whereas typical controller uses optocoupler from secondary
- operates in quasi-resonant mode, as opposed to continuous / discontinous operation mode

Although these two features are not essential for this project, for educational purposes it was deemed reasonable to investigate it further as it was available.

6.1 Operation principle of controller

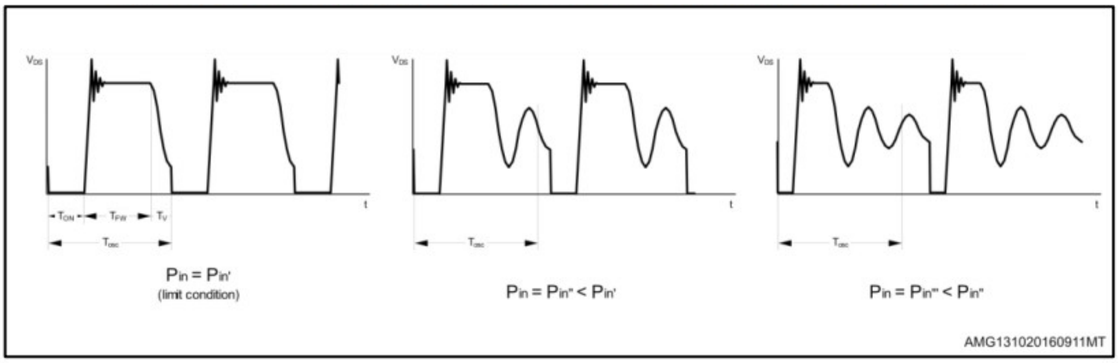

Figure 9. Drain waveform in quasi-resonant mode[6].

The controller designed for quasi-resonant operation means that switching element starts conducting when VDS is at its lowest point (valley) of the current ringing cycle. Ringing starts on transformer secondary windings as soon as transformer has transferred all the energy stored within. The ringing cycle on which the switching occurs is chosen from feedback - delay between pulses (more specifically, between turn-on events) is set in relation to output to keep the output voltage at nominal. Same applies for switch on-time.

Parasitic capacitance causes additional current when switching element starts conducting [7]. This results in switching losses. This additional current is in relation with switching element source-drain voltage.

As for the feedback of output voltage, it is sampled prior to falling of feedback winding voltage. This is better described on Figure 10.

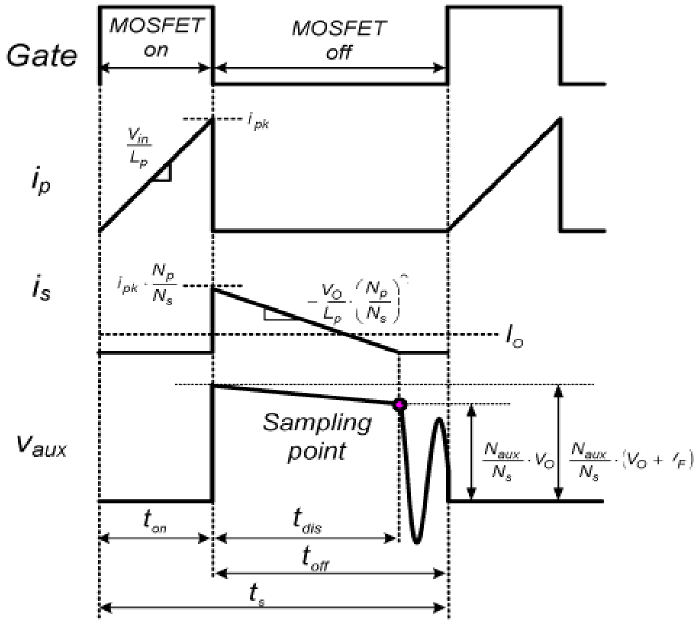

Figure 10. Example waveforms of feedback in quasi-resonant controller [8].

In regards to the output, controller is operated in constant voltage (CV) mode.

7 Calculation of transformer

As the typical application for the controller used receives output voltage from feedback (auxiliary) winding, this requires attention during transformer design for best results.

This mainly dictates that the coupling of windings shall be as good as possible. After energy stored in transformer gap is transferred to output capacitors, the voltage indicated on feedback winding represents output voltages as accurately as possible.

Leakage inductance, where any part of winding is not directly coupled to other windings, reduces efficiency of coupling [9]. As lacking coupling between secondaries is a major cause of poor cross-regulation (meaning characteristic of multiple outputs to track each other's voltages), this is further amplified as an issue due to using auxiliary winding for feedback [10].

Coupling between secondaries is improved by reducing separation distance between windings and interleaving them, which consists of splitting winding into multiple sections and applying sections in sequence [11] [12]. The latter option shall not be used unless prototype shows remarkable necessity for it, as it will add increased cost for transformer production (in the form of extra step during manufacturing). It can be viewed as adding an extra winding. As this thesis covers a fairly low-powered supply, this approach is deemed not practical and not covered in depth. For higher powered supplies, it may be beneficial as split primary allows for lower snubber losses by reducing leakage inductance of primary winding, which in turn reduces amplitude of ringing [13].

For both options isolation is a key-factor. Although coupling between secondaries and primary is less critical (resulting only in losses, not output voltage accuracy), coupling between secondaries and feedback is important. It should be pointed out, that auxiliary should be somewhat considered a primary, as the ground potential is related to mains. Therefore, one can estimate some difficulties from coupling here.

For coupling between secondaries isolation is not as critical, as only functional isolation is required.

7.1 Choice of bobbin and core

Based on multiple application notes by component manufacturers (e.g. Infineon and

Texas Instruments) on the topic of flyback converter design and flyback converter transformer design, it was determined that for 8.8 W power supply E19 or E20 transformer core is suitable [14]. Final choice of E20 was due to better availability of gapped cores through well-known retailers (Farnell, Mouser etc).
For core material initially no choice is made, but three candidates are 3F3 by Ferroxcube, PL-7 by Samwha and N87 by TDK, as they are fairly similar in their features:

Table 3. Ferrite material comparison.

Ferrite type	**Saturation flux density**	**Recommended operation frequency**
3F3	370 mT	500 kHz
PL-7	390 mT	200 kHz
N87	390 mT	500 kHz

As the chosen controller has upper frequency limit of 166 kHz, all these are suitable. During calculation of transformer, maximum flux density must be kept below saturation flux density with good tolerance. Saturated inductor (flyback transformer primary) loses all inductance and has only resistive parameter, likely to result in a destructive failure and/or fire.

Mentioned before, the gap of the transformer is essentially the primary location for energy storage during conversion [15]. Changes in core gap size affect core's A_L factor. For example, an outtake from E 20/10/6 datasheet regarding N87 [16]:

Gapped

Material	g mm	A_L value approx. nH	μ_e	Ordering code ** = 27 (N27) = 87 (N87)
N27, N87	0.09 ±0.01	363	415	B66311G0090X1**
	0.17 ±0.02	227	259	B66311G0170X1**
	0.25 ±0.02	171	195	B66311G0250X1**
	0.50 ±0.05	103	118	B66311G0500X1**

The A_L value in the table applies to a core set comprising one ungapped core (dimension g = 0) and one gapped core (dimension g > 0).

Figure 11. Gap to AL factor from N87 E20 datasheet.

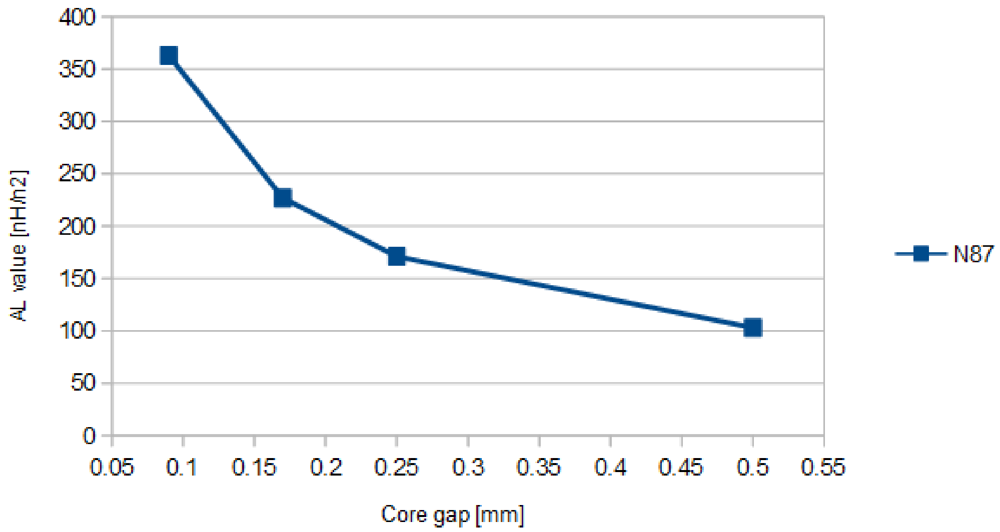

Figure 12. Core gap in relation to AL value.

When designing a transformer, A_L factor translates to inductance per turn by the following formula [17]:

$$L = n^2 \cdot A_L \tag{5}$$

where L is inductance, n is the amount of turns and A_L represents A_L factor of the core.

7.2 Calculation of windings

To prepare for calculation, known input parameters shall be listed. First calculation is performed with 3F3, due to lowest saturation flux density (most critical of the three).

Due to availability of sufficient computing power, all the necessary formulas are entered to OpenOffice Calc or an equivalent software and a suitable A_L value is estimated there using available options. For example, value of 227 nH/n^2 gave acceptable results.

Table 4. Initial transformer input values.

Data input				
Transformer	AL [nH/n2]	Bmax [T]	Ae [mm2]	
	227	0,37	32,1	
Switching	Vdc (max) [V]	Vdc (min) [V]	Vms (max) [V]	
Voltages	356,73	103,5	444	
Switcher	Frequency [kHz]	Maximum duty ratio [%]	I limit volt [V]	
	100	40	0,75	
Outputs	Vo [V]	Po (max) [W]	Io (max) [A]	Vd [V]
No. 1 (auxiliary)	15	1	0,0666666667	1
No. 2 (12 V)	12	5	0,4166666667	1
No. 3 (4 V)	4	4	1	1
No. 4 (N/A)	0	0	0	1
Total		10	1,4833333333	

Brief explanation for the values:

- Effective area (A_e) for E20/10/6 core is 32.1 mm^2.
- Maximum DC voltage on input capacitor is derived from 230 VAC with ±10% tolerance.
- Minimum DC voltage on input capacitor is derived from 115 VAC wth ±10% tolerance.
- Vms (max) represents target maximum voltage spike on drain.
- Maximum duty ratio is chosen to be below 50% (avoiding constant conduction mode, so that maximum of energy gets transferred) [4].
- "I limit volt" represents voltage on controller source pin triggering overcurrent protection.
- Although the outputs are self-explanatory, Vd represents expected voltage drop on output diode. These are chosen fairly pessimistically.

Flyback converter does not follow the typical transformer calculation method, where turns ratio is directly related to input-output voltage ratio. For relating primary to secondary, value of "ampere-turns" is used, which is acquired by multiplying winding current and winding turns. As energy does not change, the value acquired on primary is the same as expected on secondary. For example a transformer with 100 turn primary, where current is ramped up to 1 A and 10 turn secondary provides the calculation [4]:

$$100 \cdot 1(A) = 10 \cdot x(A) \tag{6}$$

Solving for x, it can be found that secondary has a current of 10 A.

Voltage wise, this gives us little to no information, as voltage is now dependant on the load. Without feedback, 10 A current pulses on a 12 V rail (which is specified for up to 0.4 A) will quickly raise the voltage to unaccpetable levels. With no experience, even 10 A pulse itself can sound violent.

To put things into perspective, 40% duty cycle at 100 kHz results in 4 µs on-time per 10 µs cycle. For the sake of argument, we can consider the transformer (inductor) discharge time same. Estimating a fairly small output capacitor of 100 µF and no load, according to the formula covering voltage change on capacitor in relation to capacitance, voltage and time:

$$i = C \frac{\Delta V}{\Delta t} \tag{7}$$

$$\Delta V = \frac{i \cdot \Delta t}{c} = \frac{10 \cdot 4 \cdot 10^{-6}}{100 \cdot 10^{-6}} = 0.4(V) \tag{8}$$

As feedback voltage is checked every cycle, 0.4 V rise per cycle can be acceptable ripple, although in reality additional capacitance value may be reasonable and there is likely to be some load available.

Having set in place the parameters for maximum input voltage and maximum voltage stress on switching element, turn ratios can be determined using the following formula:

$$\overline{V_{ms}} = \overline{V_{dc}} + \frac{N_p}{N_{sm}} (V_o + V_f) \tag{9}$$

$$\frac{N_p}{N_{sm}} = \frac{\overline{V_{ms}} - \overline{V_{dc}}}{V_o + V_f} \tag{10}$$

$$\frac{N_p}{N_{sm1}} = \frac{444 - 356.73}{15 + 1} = 5.454375 \tag{11}$$

$$\frac{N_p}{N_{sm2}} = \frac{444 - 356.73}{12 + 1} = 6.713076923 \tag{12}$$

$$\frac{N_p}{N_{sm3}} = \frac{444 - 356.73}{4 + 1} = 17.454 \tag{13}$$

where $\overline{V}_{ms}$ represents target maximum voltage spike on drain, $\overline{V}_{dc}$ represents maximum DC voltage in, N_p/N_{sm} represents primary to secondary turn ratio, V_o represents nominal output voltage of respective secondary and V_f represents respective secondary's rectifier forward voltage.

To verifying that core does not saturate, it is necessary to calculate core reset time necessity. To ensure discontinous mode, 20% of cycle is left for dead-time. Therefore, with previously chosen 40% maximum on-time leaves us 40% of cycle for core reset (40% of 10 µs or 4 µs). To test if the maximum duty cycle is suitable for the application, the following formula is used:

$$(\underline{V}_{dc} - V_{sf})\overline{T}_{on} = (V_o + V_f)\frac{N_p}{N_{sm}}\underline{T}_r \tag{14}$$

$$\underline{T}_r = \frac{(\underline{V}_{dc} - V_{sf})\overline{T}_{on}}{(V_o + V_f)\frac{N_p}{N_{sm}}} \tag{15}$$

where $\underline{V}_{dc}$ represents minimum DC voltage in, V_{sf} represents switching element voltage drop while conducting, $\overline{T}on$ represents maximum on-time, V_o represents nominal output voltage of respective secondary, V_f represents respective secondary's rectifier forward voltage, N_p/N_{sm} represents primary to secondary turn ratio, and T_r represents minimal necessary core reset time.

Following this formula, 4 µs on-time of 10 µs cycle requires ~4.70 µs for core reset. This step deems it necessary to reduce maximum duty-cycle. Recalculating previous formulas, closest suitable integer is 36%, resulting in 3.6 µs on-time and 4.4 µs core reset time.

Primary inductance can now be derived as along with maximum output load other parameters have been determined. The formula for primary inductance is derived from output voltage in relation to load formula [4]:

$$V_o = \underline{V}_{dc}\overline{T}_{on}\sqrt{\frac{R_o}{2.5 T L_p}} \tag{16}$$

where V_o represents output voltage, $\underline{V}_{dc}$ represents minimum DC input voltage, $\overline{T}_{on}$ represents maximum on-time, R_o represents output load, T represents cycle period and L_p represents primary inductance.

Primary is calculated for limit case of lowest input voltage (resulting in highest on-time for same output power) and maximum output power. As primary is indifferent to the amount of secondaries, Vo and Ro can be substituted with total output power resulting in following formula:

$$L_p = \frac{R_o}{2.5\,T}\left(\frac{\underline{V}_{dc}\overline{T_{on}}}{V_o}\right)^2 = \frac{\left(\underline{V}_{dc}\overline{T_{on}}\right)^2}{2.5\,T\,\overline{P_o}} = \frac{103.5\cdot\left(3.6\cdot 10^{-6}\right)^2}{2.5\cdot 10^{-6}\cdot 8.8} = 555.32\,(\mu H) \tag{17}$$

where R_o represents output load, T represents cycle period, $\underline{V}_{dc}$ represents minimum DC input voltage, $\overline{T}_{on}$ represents maximum on-time, V_o represents output voltage and $\overline{P}_o$ represents maximum output power.

With maximum on-time, inductance and minimum input voltage drain peak current for limit case is calculated:

$$I_{peak(primary)} = \Delta I = \frac{V\cdot\Delta T}{L} = \frac{103.5\cdot 3.6\cdot 10^{-6}}{555.32\cdot 10^{-6}} = 0.671\,(A) \tag{18}$$

where ΔI is change in current (starting from core reset, where current is zero), V is voltage applied to inductor (minimum input voltage) and ΔT is period of application of potential (maximum on-time).

Resulting peak value for primary current is well below the maximum drain current of 1 A for Altair05T-800. As this calculation does not take into account voltage drop on components, in reality the peak value is lower.

At this point it is also reasonable to calculate overcurrent protection shunt value. Protection is triggered when voltage on shunt (in series with path to ground) has risen to 0.75 V (typical, with respective values with tolerances being at 0.70 V and 0.80 V, stated by the manufacturer). The ideal shunt would be1.1178 ohms, however finding precisely this value among widely available components is not very likely. For component availability reasons this is rounded to 1.0 ohm with a reasonable tolerance of ±5% or better. To be safe, worst case scenario shall be calculated with 0.80 V triggering voltage and 0.95 ohm resistor for current and resistor power dissipation.

$$I_{prot}\,max = \frac{0.80}{0.95} = 0.84\,(A) \tag{19}$$

Even with the tolerances the values are below the limit.

It should be noted that currently only peak current for primary winding has been determined. For estimation of dissipation, the RMS value needs to be estimated. It is estimation instead of calculation, as the resistance of the winding is not available at this moment.

As RMS of sawtooth is calculated according to the formula:

$$I_{RMS(sawtooth)} = \frac{I_A}{\sqrt{(3)}} \tag{20}$$

where $I_{RMS\text{-}SAW}$ represents RMS current of sawtooth and I_A represents amplitude of waveform.

This formula being valid for sawtooth, duty cycle needs to be taken into account to be valid for flyback primary. Therefore:

$$I_{RMS(primary)} = \frac{I_{peak}}{\sqrt{(3)}} \cdot \sqrt{\left(\frac{T_{on}}{T}\right)} = \frac{0.671}{\sqrt{(3)}} \cdot \sqrt{\left(\frac{3.6\,\mu s}{10\,\mu s}\right)} = 0.2324276446\,A \tag{21}$$

With RMS value available, shunt resistor power can be determined:

$$U_{shunt(max)} = I_{RMS(primary)} \cdot R_{shunt(max)} = 0.2324276446 \cdot 1.05 = 0.24404902683\,(V) \tag{22}$$

$$P_{RMS(shunt)} = I_{RMS(primary)} \cdot U_{shunt(max)} = 0.05672374\,(W) \tag{23}$$

Although the power of 56 mW is insignificant in this application and could be dissipated by a 0402 (imperial size) resistor, the peak current should be taken into account and resistor chosen to withstand the necessary current [18].

Returning to transformer design, turns can now be calculated as primary inductance and turn ratios between windings are available:

$$L = n^2 \cdot A_L \tag{24}$$

$$n = \sqrt{\left(\frac{L}{A_L}\right)} \tag{25}$$

$$n_{primary} = \sqrt{\left(\frac{L_p}{A_L}\right)} = \sqrt{\left(\frac{555.32304 \cdot 10^{-6}}{227 \cdot 10^{-9}}\right)} = 49.46066118 \tag{26}$$

Attention should be drawn to the point, that the resulting value is quite the opposite of an integer. Winding half of a turn on transformer can be achieved, but it is additional work which is not reasonable. For this value, 49 or 50 give fairly similar results, so 49 was chosen as it is not critical, however for secondaries, where smaller number of turns (e.g. < 10) is likely, it should be considered.

The secondaries can also be calculated from primary turns value and turns ratios:

$$\frac{N_p}{N_{sm}} = const \tag{27}$$

$$N_{sm} = \frac{N_p}{const} \tag{28}$$

$$N_{sm1} = \frac{555.32304}{5.454375} = 9.06807126 \tag{29}$$

$$N_{sm2} = \frac{555.32304}{6.713076923} = 7.367807899 \tag{30}$$

$$N_{sm3} = \frac{555.32304}{17.454} = 2.833772269 \tag{31}$$

Knowing the application for power supply, 12 V winding (N_{sm2}) shall be rounded to 7 turns and 4 V winding (N_{sm3}) to 3 turns. The reasoning behind this is that relays, which are the only consumers on 12 V rail are indifferent to slightly lower voltage, however higher voltage causes unnecessary heating and 4 V rail is used to drop it down further to 3.3 V, so additional margin is welcome, whereas reducing the margin may render the 3.3 V rail unstable.

Final unknown value is the minimal wire thickness for windings. To calculate this, only RMS for all secondaries is needed. Skin effect shall also be taken into account. Therefore, it is likely that one winding requires multiple strands of wire to be effective at higher frequencies.

Controller frequency is top limited to 166 kHz, therefore the skin effect calculation shall be based on this. Regardless of actual current, it can be calculated what is the maximum surface area for conductor at this frequency. All calculations are based on copper windings ($\rho = 1.68 \cdot 10^{-8}$ ohm·m):

$$\delta = \sqrt{\left(\frac{\rho}{\pi \cdot f \cdot \mu}\right)} = \sqrt{\left(\frac{1.68 \cdot 10^{-8}}{\pi \cdot 1.66 \cdot 10^{5} \cdot 4 \cdot \pi \cdot 10^{-7}}\right)} = 0.160110837 (mm) \tag{32}$$

where δ is skin depth, ρ is bulk resistivity and μ permeability constant.

Considering skin depth to be maximum effective radius and wire perfect circle, thickest usable wire shall be [19]:

$$d=2\cdot r=2\cdot 0.160110837=0.320221674(mm) \tag{33}$$

$$S=r^2\cdot\pi=0.160110837^2\cdot\pi=0.80536236(mm^2) \tag{34}$$

The RMS currents for secondaries are specified.

For selection of wire thickness, tip of "circular mils required = 500 · I_{RMS}" is followed [4]. Circular mil represents surface of a circle with a diameter of 1 mil (0.0254 mm or 1/1000th of an inch). As the author of this thesis is fairly incapable of thinking in imperial units, this is calculated in multiple steps to avoid errors.

Table 5. Thicknesses of wires for windings.

Winding	**I_{RMS} in A**	**Circular mils**	**Thickness in mils**	**Thickness in mm**	**Surface area in mm^2**
Primary	0.23243	116.21500	10.78031	0.27382	0.05889
Secondary 1 (auxiliary)	0.06667	33.33500	5.77365	0.14665	0.01689
Secondary 2 (12 V)	0.41667	208.33500	14.43381	0.36662	0.10556
Secondary 3 (4 V)	1.00000	500.00000	22.36068	0.56796	0.25335

As can be seen, primary and secondary 1 can be wound with single wire, however for secondary 2 and 3 multiple wires are required. Assuming maximum of 0.3mm thickness wire is used due to skin effect limitations, two parallels are suitable for both.

This concludes the calculations for transformer from electrical point of view.

Table 6. Transformer windings details.

Winding	**Turns**	**Wire diameter in mm**	**Parallels**
Primary	49	0.3	1
Secondary 1 (auxiliary)	9	0.2	1
Secondary 2 (12 V)	7	0.3	2
Secondary 3 (4 V)	3	0.3	2

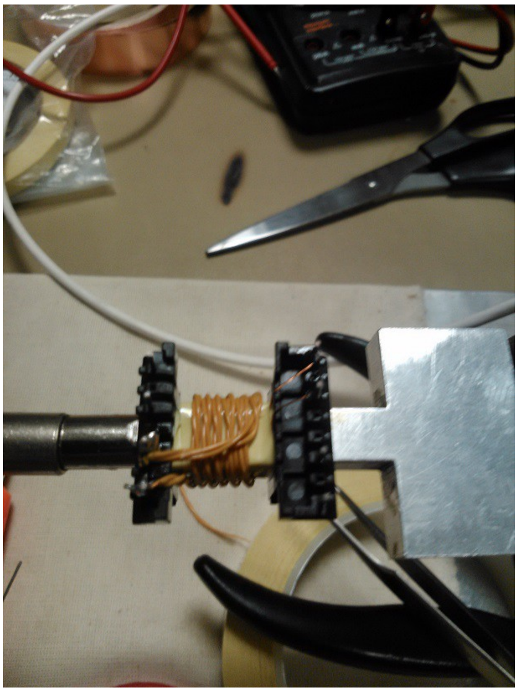

Figure 13. Example of multiple intertwined parallels from a testing transformer.

Where multiple parallels were specified, length of wire required was estimated with additional margin for error, cut into lengths and intertwined prior to winding to keep the currents induced in winding wires as similar as possible.

8 Snubber

Initially it was planned to use a non-dissipative snubber [20].

As the development for non-dissipative snubber was deemed more complex and time consuming it was moved to "optional improvement" category. It was further justified by the low power of the power supply, hence power dissipated on snubber does not cause remarkable issues. Further design followed methods used for classical RCD snubber, described in Figure 14.

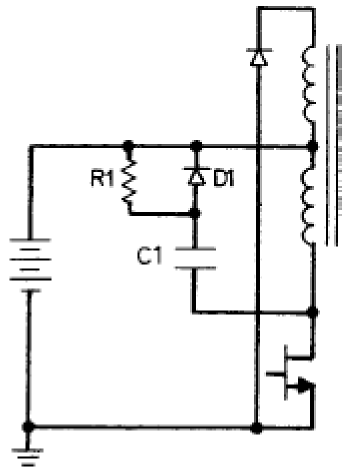

Figure 14. RCD snubber example.

When referring to example from Figure 14. RCD snubber example., it should be noted that only one diode is used, as the primary does not have a centre-tap [4].

The snubber clamping voltage was defined prior to transformer calculation, therefore diode's maximum repetitive reverse voltage requirement can be determined already (V_{ms} -V_{DC}), however capacitor and resistor values are still unknown. To calculate this, leakage inductance of primary is required. Although this is unknown until actually winding the transformer, it can be estimated to be roughly 3% of winding [21].

$$L_{leak(primary)} = 0.03 \cdot L_p = 0.03 \cdot 555.32304 = 16.66(uH) \quad (35)$$

Estimated power dissipated on snubber:

$$P_{snubber} = \frac{1}{2 \cdot L_{leak(primary)} \cdot I^2_{peak(primary)} \cdot \frac{1}{T}} = \frac{1}{2 \cdot 16.66 \cdot 10^{-6} \cdot 0.671^2 \cdot 100 * 10^3} = 45(mW) \quad (36)$$

These can be used to calculate suitable resistor and absolute minimum capacitor:

$$R_{snubber} = \frac{\left(V_{ms} - \overline{V_{dc}}\right)^2}{P_{snubber}} = \frac{\left(444 - 356.73\right)^2}{0.045} = 169.245\left(kOhm\right) \quad (37)$$

$$C_{snubber} \gg \frac{1}{\frac{1}{T} \cdot R_{snubber}} = \frac{1}{100 \cdot 10^3 \cdot 169245} = 59.09\left(pF\right) \quad (38)$$

This leaves fairly free interpretation of the capacitor value. For example, 1200 pF satisfies the formula.

9 Filtering

Filtering comprises of common-mode and differential-mode. The basic topology can be seen in Figure 15 [22].

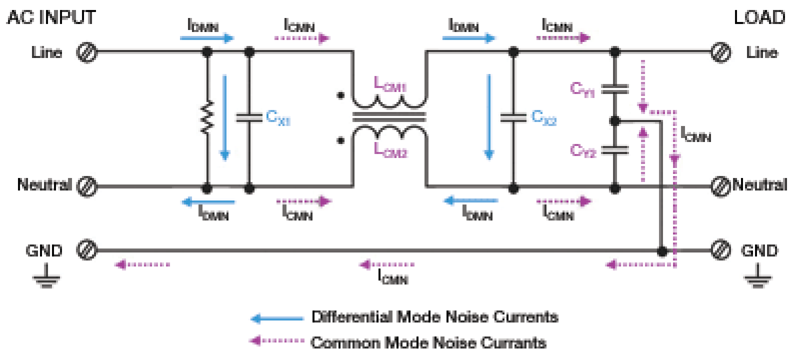

Figure 15. Filtering layout.

Primary applicable standard for the end product (in this section referred to as "primary standard") is EN 60730-1:2012.

Necessary limits for filtering and measurement methods are obtained from EN 55022:2011, which is referred to by the primary standard.

Device shall be tested for class B ITE, for which the applicable limits are more strict.

As the standards mentioned are not available for free, the values are not copied to this thesis due to legal and ethical reasons.

This thesis attempts to cover only the conducted-emissions, as this can be measured to an extent with fairly simple tools (e.g. LISN and spectrum analyzer), whereas radiated emissions require an anechoic chamber.

9.1 Common mode

Common mode filtering is primarily achieved by the common-mode choke installed in the input of the power supply. Although the necessity and specific frequency ranges necessary to attenuate are uncertain until first tests, it can be assumed that most of the noise shall occur around switching frequency (~ 100 to 200 kHz).

The placeholder choke is SU9V-07010 by Kemet.

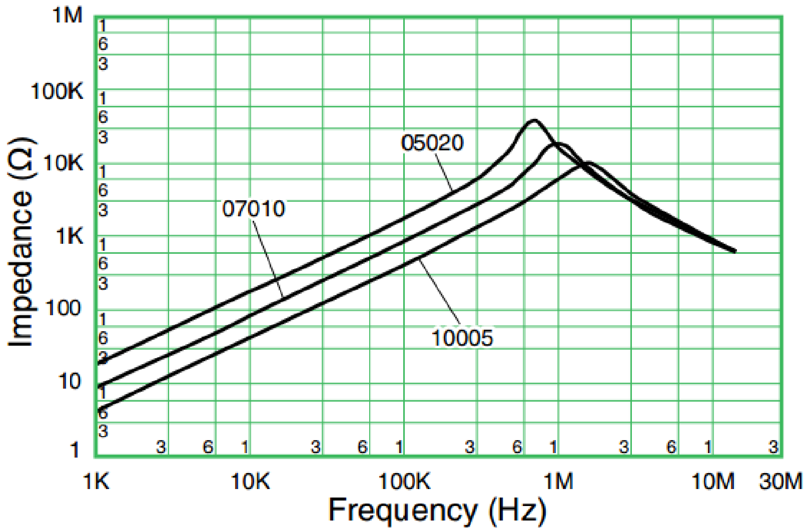

Figure 16. Common-mode choke frequency characteristic.

The frequency characteristic available from manufacturer datasheet shows that although primary surpression is provided at frequency around 1 MHz, there is significant attenuation available at 100 kHz as well [23].

Although unlikely with a low-power device as described in this thesis, additional common-mode filtering can be achieved by applying Y-capacitors between protective earth and mains input on the power-supply side of the common-mode choke.

Limits for quasi-peak and average values (for both current and voltage) for common-mode conducted noise can be found in EN 55022:2011 table 4.

9.2 Differential mode

Aside from the inevitable DC-link capacitor (the capacitor mounted between diode-bridge output and power-section input), X-capacitors are mounted across the line inputs prior and post the common-mode choke. This shall surpress any noise that is generated by the power supply and subjected to only one of the input lines.

Shall this be deemed insufficient, DC-link capacitor can be changed to C-L-C low-pass filter. During prototyping, it might cause extended wires to mount it, but it should be noted that for C-L-C filter additional (even parasitic!) inductance can be welcome.

Limits for quasi-peak and average of differential-mode conducted noise can be found in EN 55022:2011 table 3.

10 Power factor correction

Due to the diode-bridge and capacitor input of the power supply, it is obvious that the input current waveform is not likely to be a perfect sine wave. To keep the mains network output in the expected shape, limits have been put place as to how all mass-manufactured products must behave with it.

Along with the conducted-emissions noise, power factor is also taken into account. For a perfectly resistive load the current and voltage waveforms match in all but amplitude (which is possible, but not required), resulting in an unity power factor (PF = 1). After a phase shift is introduced (e.g. by an inductive load or a capacitive load), displayed on Figure 17, power factor starts to drop [24].

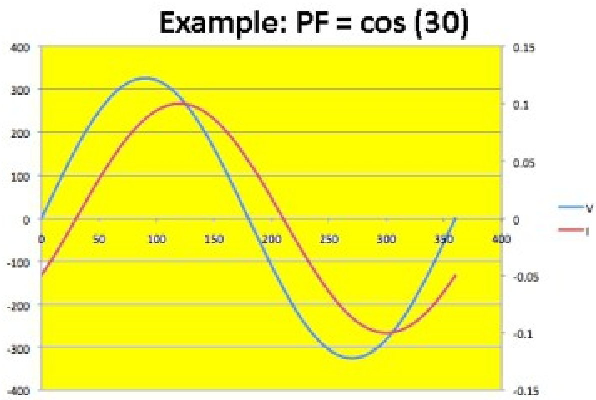

Figure 17. Example of non-unity power factor.

The issue is further complicated when taking into account the rectifiying and filtering. As the DC-link capacitor attempts to hold stable voltage, it is only charged (and input current is available) when input voltage waveform exceeds voltage on capacitor (and diode-bridge voltage drop). Result is current waveform not following the expected sinusoidal waveform, but instead having periodic peaks. With high current load and some resistance in input power it can also spoil the sinusoidal shape of the input voltage - depending how the resistance is set up by electrical wiring, it can affect other devices on same network too.

Primary applicable standard for the end product is EN 60730-1:2012, which leads to EN 61000-3-2:2006 (superseded by EN 61000-3-2:2014) where it can be found that for devices with rated power of 75 W or less (except lighting equipment) harmonic current limits do not apply.

11 Initial prototype

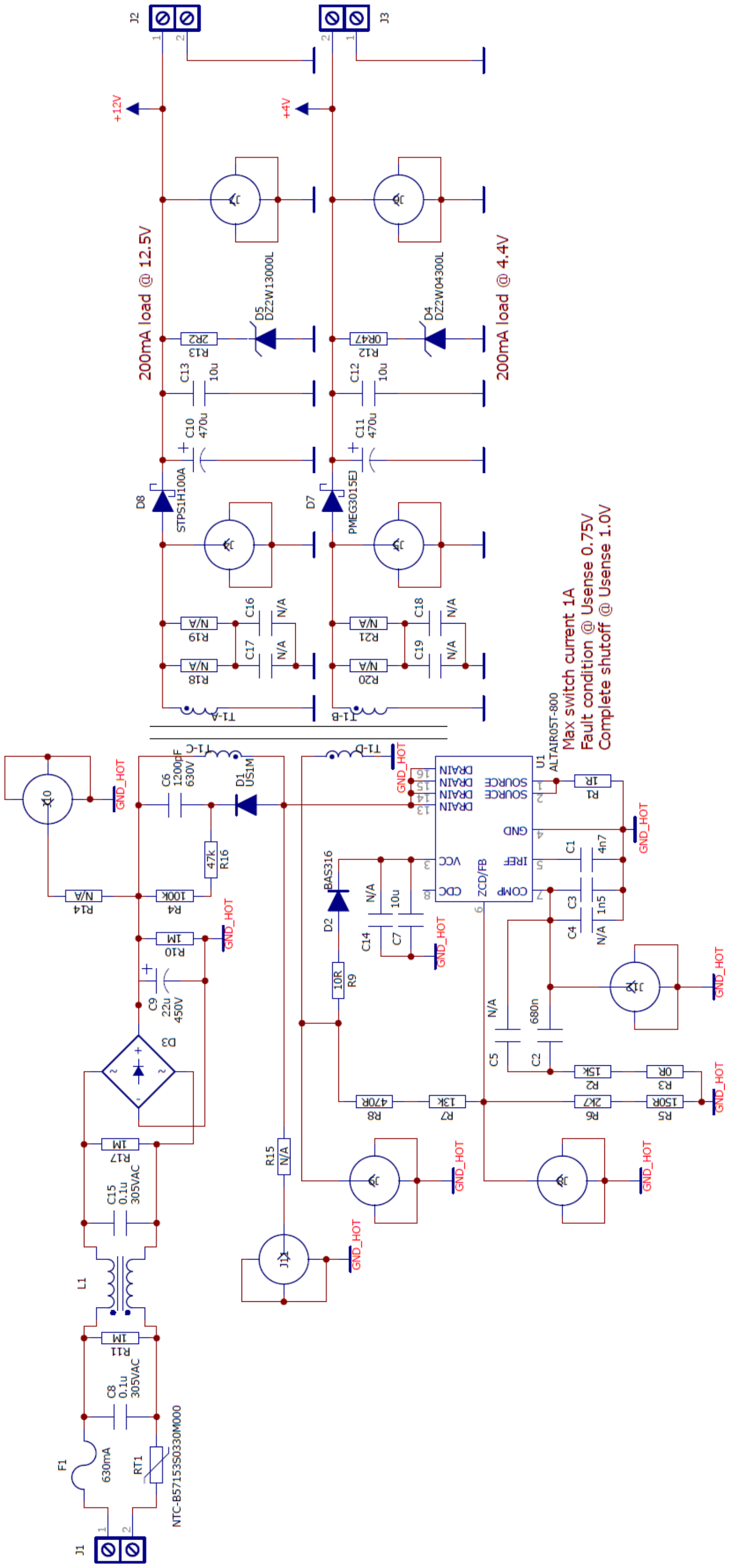

Figure 18. Schematic of initial prototype.

Initial prototype followed manufacturer recommended design where possible, using the aforementioned transformer.

Where higher capacitance was deemed necessary, electrolytic capacitors were used (e.g. C10 and C11). For lower values (typically for current surges) multilayer ceramic capacitors were used. For the latter, it should be noted that all values over 1 uF are specified with specific model in mind due to DC bias. For example, 10 µF (used in both outputs, e.g. C12 and C13) was chosen C3225X7S1H106K250AB by TDK (voltage rating of 50 V).

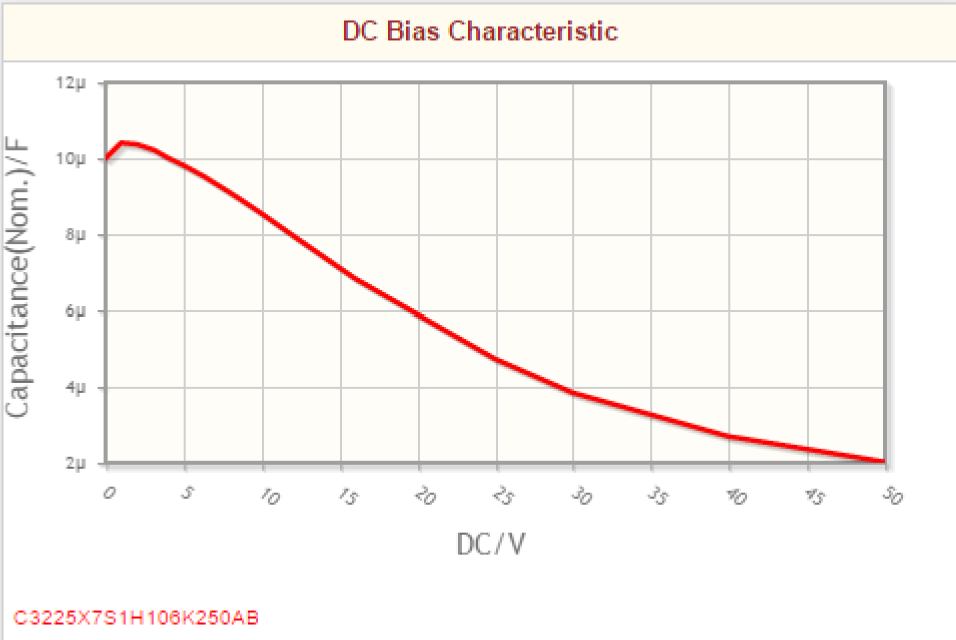

Figure 19. C3225X7S1H106K250AB DC bias graph.

DC bias graph, provided in Figure 19 show that for the voltages used (nominally 12, 4 and for auxiliary also 15 VDC), this capacitor provides roughly at least 75% of its nominal value [25].

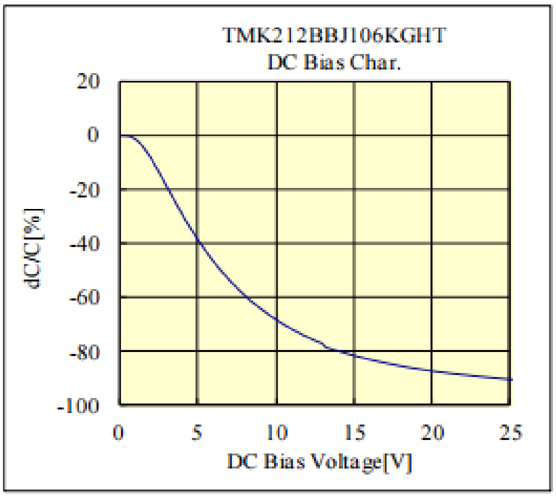

Figure 20. TMK212BBJ106KGHT DC bias graph.

To compare, TMK212BBJ106KGHT by Taiyo Juden (voltage rating 25 V) has remarkably poorer performance in same application.

Figure 20 shows that at 15 VDC 80% of the capacitance rating is no longer valid, resulting in "2 µF capacitor" [26]. For the output, where electrolytic capacitor assists the ceramic, this might be acceptable, but as can be seen from the schematic, controller's own supply is smoothed by a single ceramic capacitor.

To protect outputs (load and capacitors) clamping zeners (D4 and D5) are applied to limit output voltages. As described on the schematic, nominal loads of 200 mA are created when 12 V and 4 V rails raise to 12.5 V and 4.4 V respectively. For most of the tests, these were not assembled and should be considered unmounted unless specifically stated otherwise.

All strategic points monitoring of which may provide useful information while testing were equipped with Hirose U.FL connectors (e.g. J9 on feedback winding), allowing shielded connection to oscilloscope, effectively assisting in removing noise where low-voltage and/or high-speed signals are expected.

Component pads are available for secondary snubbers (C16 through C19 and R18 through R21), although unpopulated as their necessity is unknown prior to testing. Pads are added for convenience and to reduce unexpected parasitics.

The diodes chosen for output rectification (D7 and D8) were of Schottky kind. Schottky

type was chosen mainly due to faster recovery time (compared to regular, or even "fast-recovery" Si diodes) and lower voltage drop while forward-biased [27]. This is a frugal way to reduce losses. With the output current up to 1 A, voltage drop of silicon-based diode (circa 0.6 to 0.7 V) can cause power loss of 0.7 W, which is roughly 18% of the rated output power for single output. This estimation is based on purely DC current. When taking into account the switching, recovery-time introduces more losses [28]. Higher currents, necessary to keep the RMS current to previously mentioned 1 A (the continous output current) increase the forward voltage drop further.
When using Schottky diodes both causes of losses (switching based recovery losses and forward voltage drop) are diminished. It should also be noted, that as in this application the feedback is taken from output windings, voltage drop on rectifier (which is dependant on the load) causes output voltage to drop below the nominal. Adjusting transformer turns ratio to compensate this should be done for idle state only as designing the compensation for full load may damage the consumers attached to the power supply.

Aside from typical slow-blow fuse for safety (F1), NTC resistor is also included in the schematic (RT1). This is to resist the high-current surge caused by DC-link capacitor (C9) when powering up the device, which is a well known issue of mediocre quality laptop power supplies to this author.

Choosing specific diode models is based on current and maximum repetitive reverse voltage. Calculation for snubber diode (C6) is fairly simple. Previously the maximum voltage on switching element drain was set to 444.0 VDC, leading the calculations to be based on that. Minimum DC input voltage being set to 103.5 VDC leads to the difference of 340.5 VDC. Snubber can be considered an essential safety feature from the reliability view point, so over-dimensioning the rating is very welcome. The peak current will be equal to the peak current of inductor, as inductor attempts to resist any change in its current.

Calculation for the secondary diodes needs to take into account the actual transformer effect of flyback transformer, causing voltage peak on secondary winding. Voltage is not accompanied with any current, as the diode is reverse-biased and not conducting [29].

$$V_{SDRRM}=\frac{N_S}{N_P}\cdot\overline{V_{DC}}+V_O \tag{39}$$

Where V_{SDRRM} is secondary diode repetitive reverse voltage, N_S/N_P is secondary to primary turns ratio, $\overline{V}_{DC}$ is maximum DC input voltage and V_O is output voltage corresponding to the diode.

Table 7. Output diode V_{SDRRM} requirements.

Output	**V_{SDRRM} [V]**
Feedback / Controller power	81.52
12 V	63.96
4 V	34.84

Final product incorporating the power supply addressed in this thesis shall most likely be designed around a 4-layer PCB. Although the controller pinout allows for single-layer PCB, it was still deemed reasonable to use a 2-layer PCB to include an intact ground plane.

During PCB layout attention was paid to loops with high current and frequency. This covers the following loops:

- Input DC capacitor to primary winding to switching element (to input DC capacitor)
- Secondary winding to output rectifier to output capacitor (to secondary winding) (NB! Both secondaries)
- Primary winding to snubber (to primary winding)
- Secondary winding to secondary snubber (to secondary winding) (NB! Both secondaries)

The list does not contain the auxiliary winding as the currents there are insignificant and unlikely to cause any EMI or other noise.

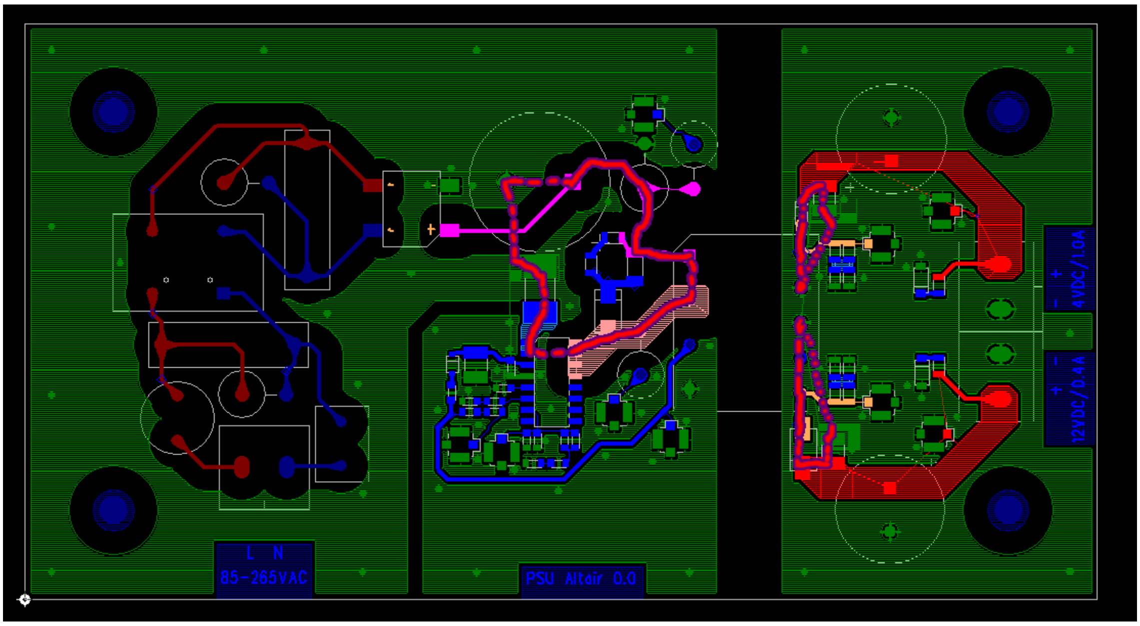

Figure 21: First prototype with operation loops highlighted

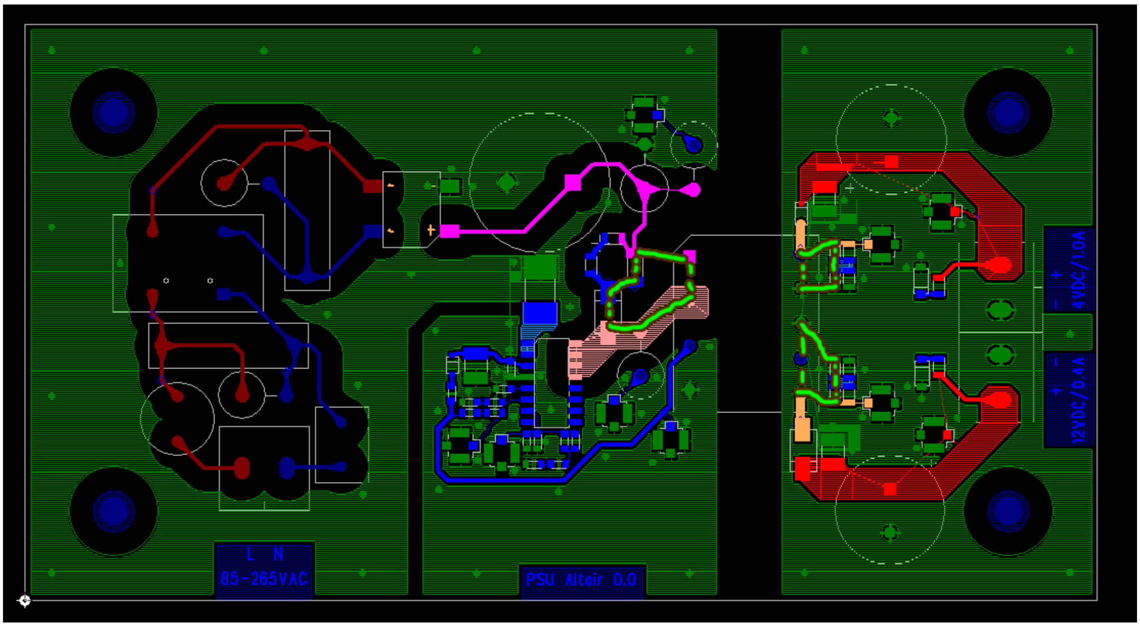

Figure 22. First prototype with snubber loops highlighted.

As can be seen from the previous illustrations, some attention has been paid to isolation gaps in copper. During prototyping excessive effort was not put into it, as the prototype was to be operated in laboratory conditions with no pollution to cause creepage, under supervision and using suitable protection devices (isolation transformer, resettable fuses).

With the prototype assembled, success was not immediate. Controller started up for very limited number of cycles (below 10). Brief investigation showed that auxiliary winding pins had been interchanged with one another. Even though it was an unwanted situation, it did demonstrate one example how the controller managed to fail safely. During the first few cycles expected feedback was not received from auxiliary winding, which caused the controller to stop switching action.

11.1 Various tests

After fixing the issue the controller started up with surprisingly little issues. It was fairly evident that the desired output load was not available. Running at 230 VAC only, as this should be more optimal (keeping primary peak current lower), best results achieved with the first transformer were 6.1 - 6.2 W for output, regardless of load division between outputs (as expected due to same magnetic core for both windings), well below the value of 8.8 W specified in problem statement. Increasing (resistive) load above the previously mentioned 6.1 - 6.2 W, controller entered into endless loop of resetting at roughly 4 Hz, with the output momentarily gaining power and immediately running out of it due to load. Where not specified, resistive load was used. This was due to constant current load causing power supply to enter protection prematurely - voltage droop on output would cause the current to increase, further decreasing voltage at output, in turn increasing current again until supply entered overload protection. To restart the supply, load had to be disabled. Resistive load does not have this issue and is in essence self-regulating, allowing for much more efficient load measurement.

Two more issues were detected in this phase:

1. Loading one output causes the other one to raise significantly
2. Quasi-resonant mode is not working

The first issue was clearly visible that while loading the 4 V output with 0.8 A using constant current load, the voltage on 12 V rail rose up to 18 V. This issue was most likely caused by careless and hurried winding of transformer as it is a textbook example of poor coupling between windings, as explained in chapter 7 Calculation of transformer. Investigating this issue was put on hold, as the power output was of highest priority.

The second issue was expected to be a more direct cause and symptom for low output power. The controller was operating completely opposite to the expected behaviour -

instead of starting its cycle at a valley, it started at a peak.

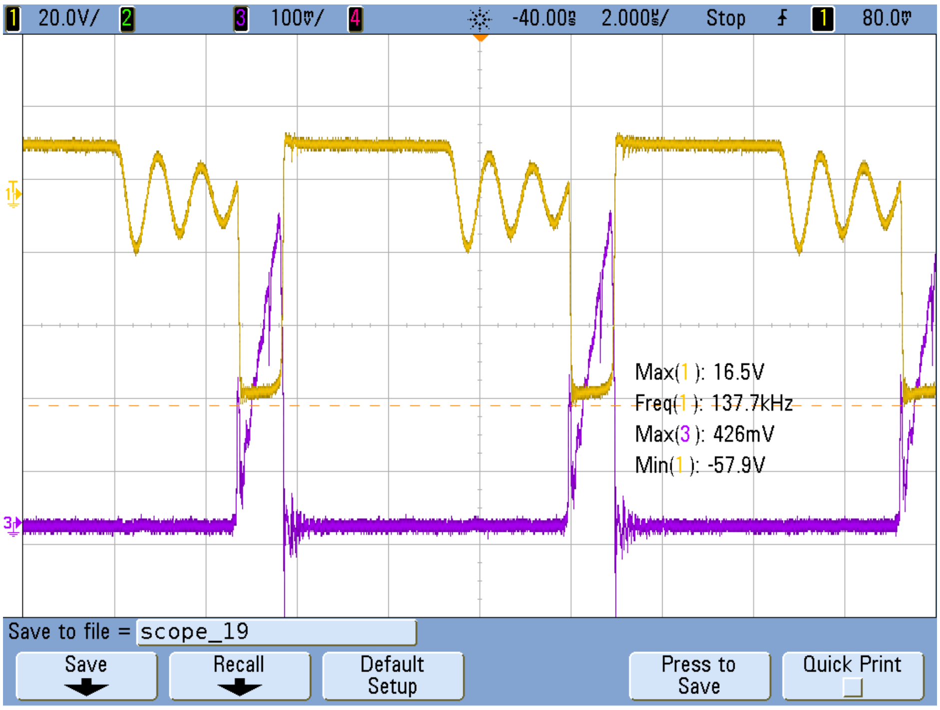

Figure 23. Failing quasi-resonant behaviour.

On the oscillogram pictured in Figure 23 yellow line represents the output of the auxiliary winding and purple line represents voltage on the current shunt. Screenshot taken while maximum possible load (~ 6 W) was applied.

As can be seen apart from the poor quasi-resonant behaviour, the voltage on current shunt does not measure up to the level that should trigger overcurrent alert. Therefore it can be safely said that too high current in primary winding is not the cause for limited output power.

The next step was to wind transformer as perfectly as possible. Winding order followed the same pattern as for initial transformer with one layer of polyester tape between windings:

1. Primary (closest to the center of the core)
2. 4 V winding
3. 12 V winding
4. Auxiliary winding

This, however, did not solve problems with quasi-resonant mode. No documentation had any mention of such behaviour, therefore one theory was that the controller was defective. To verify this the IC was replaced. Behaviour remained the same.

As another device with same controller was available that was known to be working, brief measurement on that was performed to verify the controller is actually capable of operating correctly.

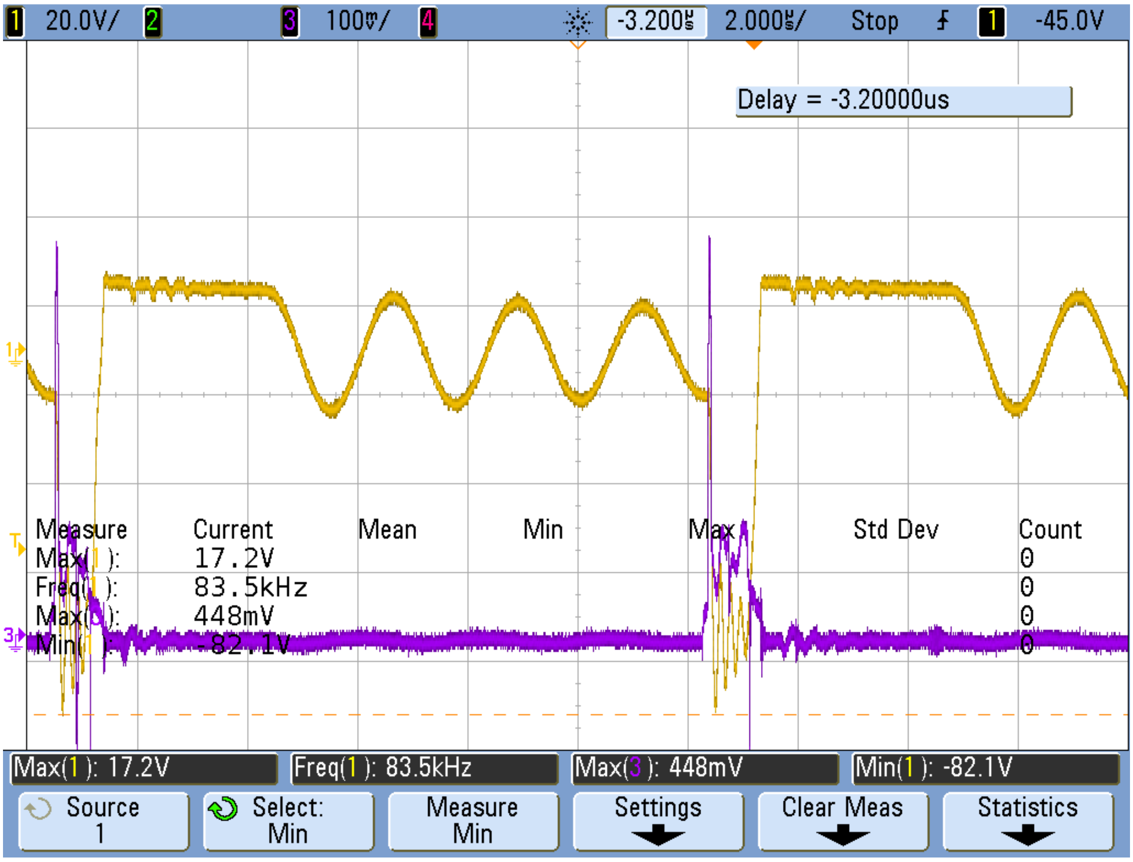

Figure 24. Controller waveform on a working example board.

Similar to previous oscillogram, yellow represents auxiliary output and purple represents primary current shunt.

As can be seen, the quasi-resonant action follows the manufacturer's description and switching cycle starts at a valley. The noise on current shunt is most likely a noise induced measurement error, as the prototype described in this thesis allowed for measuring with coaxial connectors directly from PCB, whereas the working example needed extended wires to safely access the points of interest, causing visible noise on low-voltage signals.

This lead to investigation to find the differences between example device and prototype as the quasi-resonant mode failing did not seem to be related to load. The effect was constant. Aside from output voltages the main possible difference could only be the transformer. Looking into the values calculated for prototype, the working example and reference design side-by-side, it became apparent that reference design and working example had noticeably higher primary inductance values.

Table 8. Primary inductance values.

Device	Primary inductance (nominal) [µH]
Prototype	555
Working example	4800
Reference design (by ST)	2200

No documentation had any hint that this difference could be related to the issue. As a desperate attempt another flyback transformer was scavenged from another power supply. Having only two windings (primary and a single secondary), the inductances were 2000 µH and 20 µH respectively. Using the secondary as auxiliary it was mounted to the prototype PCB. Surprisingly enough, even without any load other than controller's own power consumption, quasi-resonant mode started working as expected.

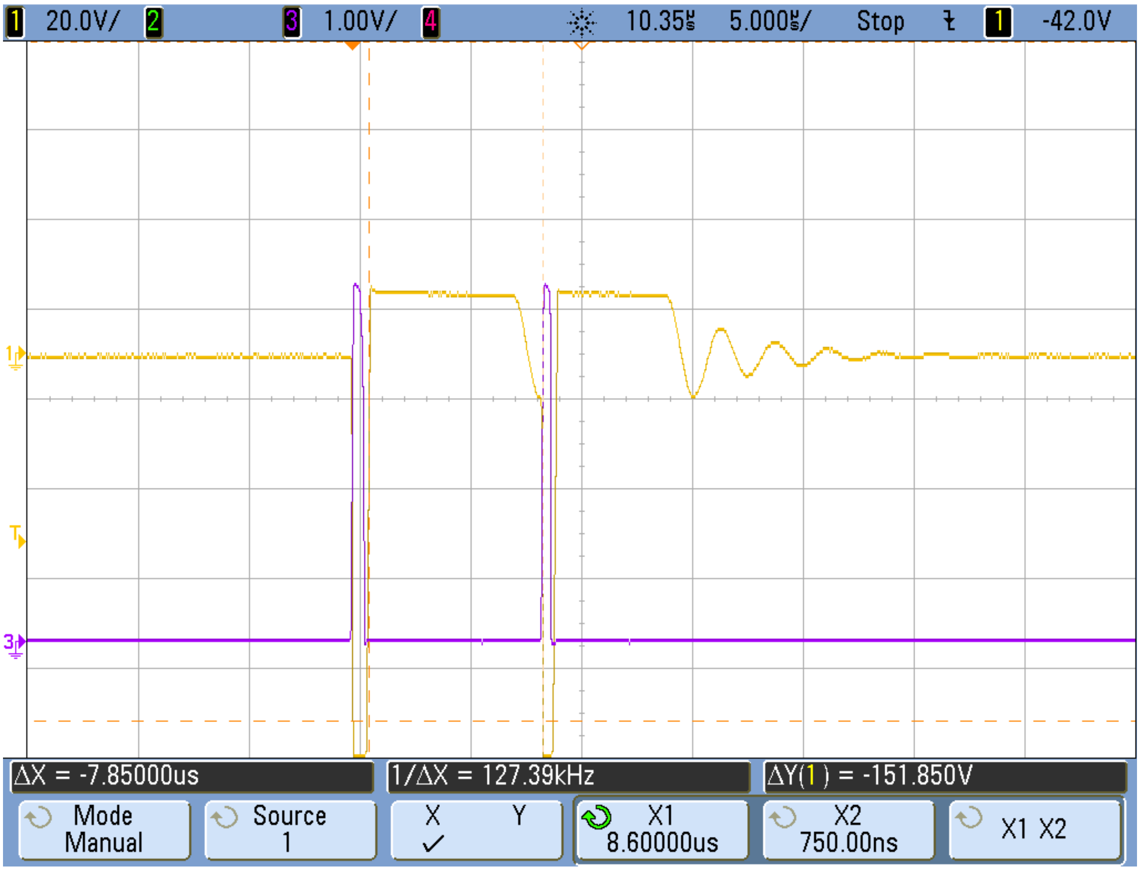

Figure 25. 2000 µH inductance in primary.

As seen, the switching cycle starts exactly at a valley. Low amount of switching cycles is explained by no load.

To further test this theory, new transformer was wound with amount of primary turns increased. It was aimed to keep turns ratio similar.

Table 9. Transformer windings for higher inductance.

Winding	Turns	Inductance (calculated / real) [µH]
Primary	107	2592 / 2539
Auxiliary	20	94 / 99
12 V	17	62 / 66
4 V	6	9 / 10

As expected, quasi-resonant mode appeared to be working as seen in Figure 26.

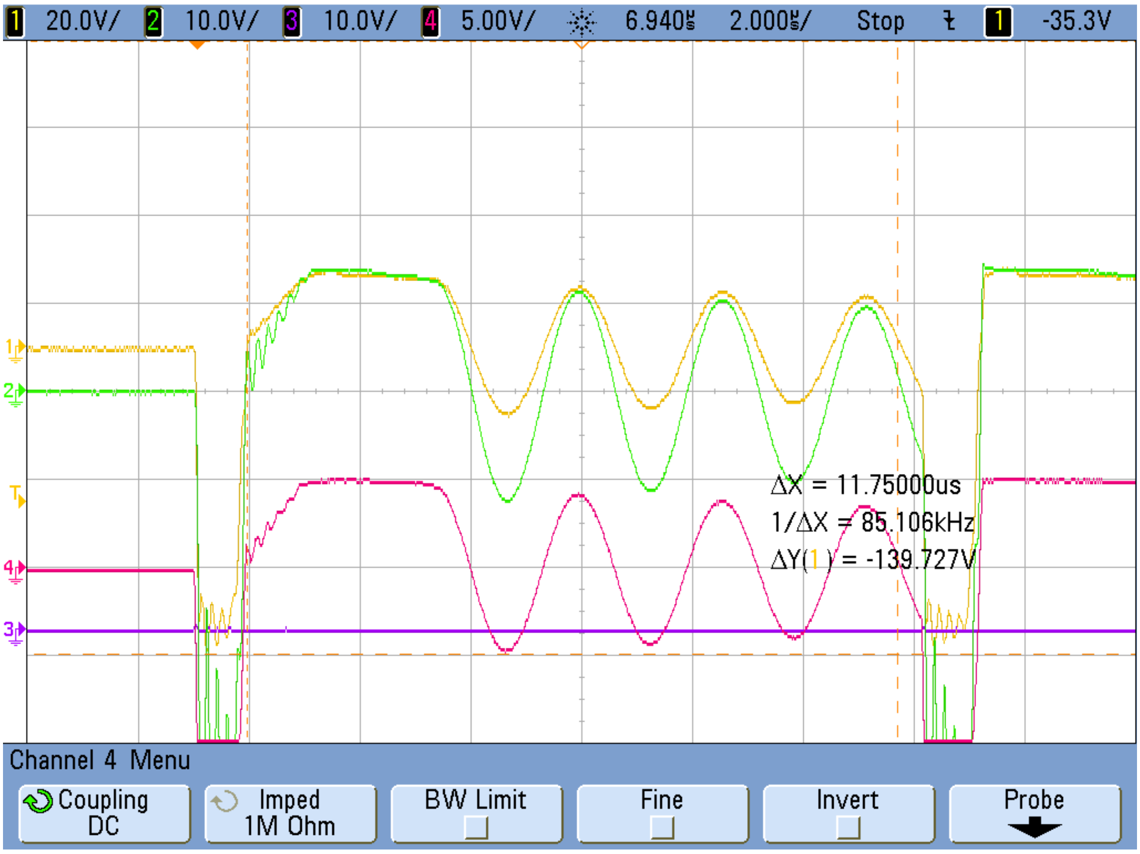

Figure 26. Waveforms after increasing primary inductance.

Aside from previously described lines (yellow for auxiliary winding and purple for current shunt), green and red represent 12 V and 4 V secondary windings respectively.

Although the controller started behaving as described in datasheet, power output did not change. Total output peaked at 6.4 W.

Running out of the hints supplied by controller documentation, even grounding the cable-drop compensation input was attempted. Although the datasheet mentions in multiple places that this may be left unconnected and floating, in one paragraph it is said it is also allowed to be grounded. With the theory of floating pin acquiring some induced noise from switching, which in turn could be causing unexpected behaviour, the pin was grounded. Absolutely no difference was observed in the behaviour.

Looking for any remaining hints available, after verifying that feedback, primary current and cable-drop compensation were well, oscilloscope was applied to compensation pin of the controller.

Figure 27. Waveforms while controller loops starting.

Figure 28. Same as figure 27, but zoomed.

The lines on the oscillograms are following:

Yellow - Auxiliary winding

Green - Auxiliary winding after voltage dividers (feedback pin of controller)

Purple - Current shunt

Pink - Compensation pin

The oscillograms show that for some reason the voltage on compensation pin starts to rise, which according to the datasheet is related to primary current limit (this can also be seen on the oscillograms).

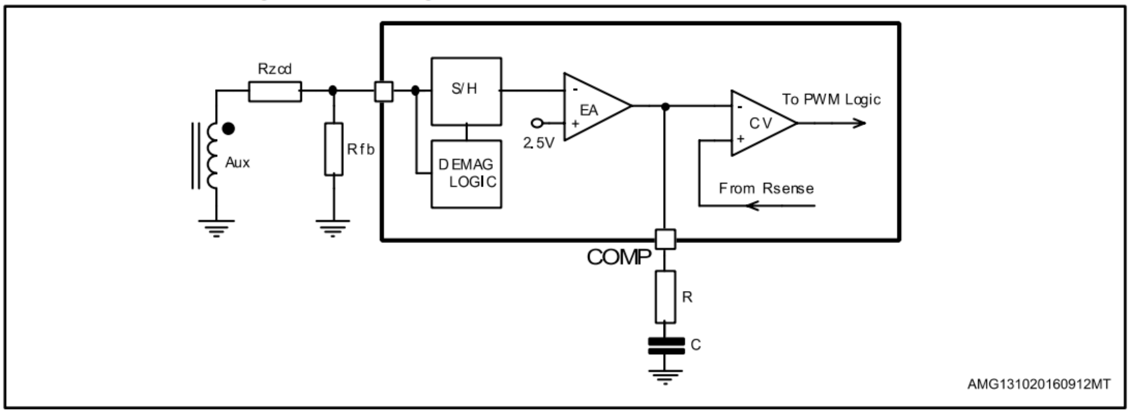

Figure 29. Voltage control principle: internal schematic, for Altair05T.

The diagram provided in Figure 29 shows that as voltage on compensation pin rises, PWM cycle is changed. This matches the oscillogram ideally. For the voltage on compensation pin to rise the only explanation is that the error amplifier (EA) should constantly have less than the reference voltage (2.5 V) on inverting input. This would mean feedback input has to suddenly drop.

Feedback can be seen from oscillogram directly from controller pin and it follows the expected waveform and amplitude precisely. The controller must have some logic for compensation that is not mentioned in the datasheet. As decapping and reverse-engineering an IC is not a part of this thesis, only reasonable step is to change the controller to something that is more reliably documented.

11.2 Lessons learned

Operating without a direct feedback from an output can be used, however it should be noted that there is not a single output that is precisely controlled. Using optocoupler to get direct readings from a single output allows for more precise output regulation. This, however, does not remove the necessity to couple the windings for multiple outputs for regulating the outputs which are not directly regulated.

If one of the primary components in the project starts to show signs of poor documentation and brief prototyping do not give the requested results, it should be considered if it is worth the risk and possibly change to a better documented component to avoid hitting a dead-end after spending significant amount of time.

This specific design, although seeming to be unusable for this application, remains still valid candidate for other applications - it may be possible that future projects need 3 W power supply and this prototype can provide that. The work done so far is not necessarily wasted.

12 Second prototype

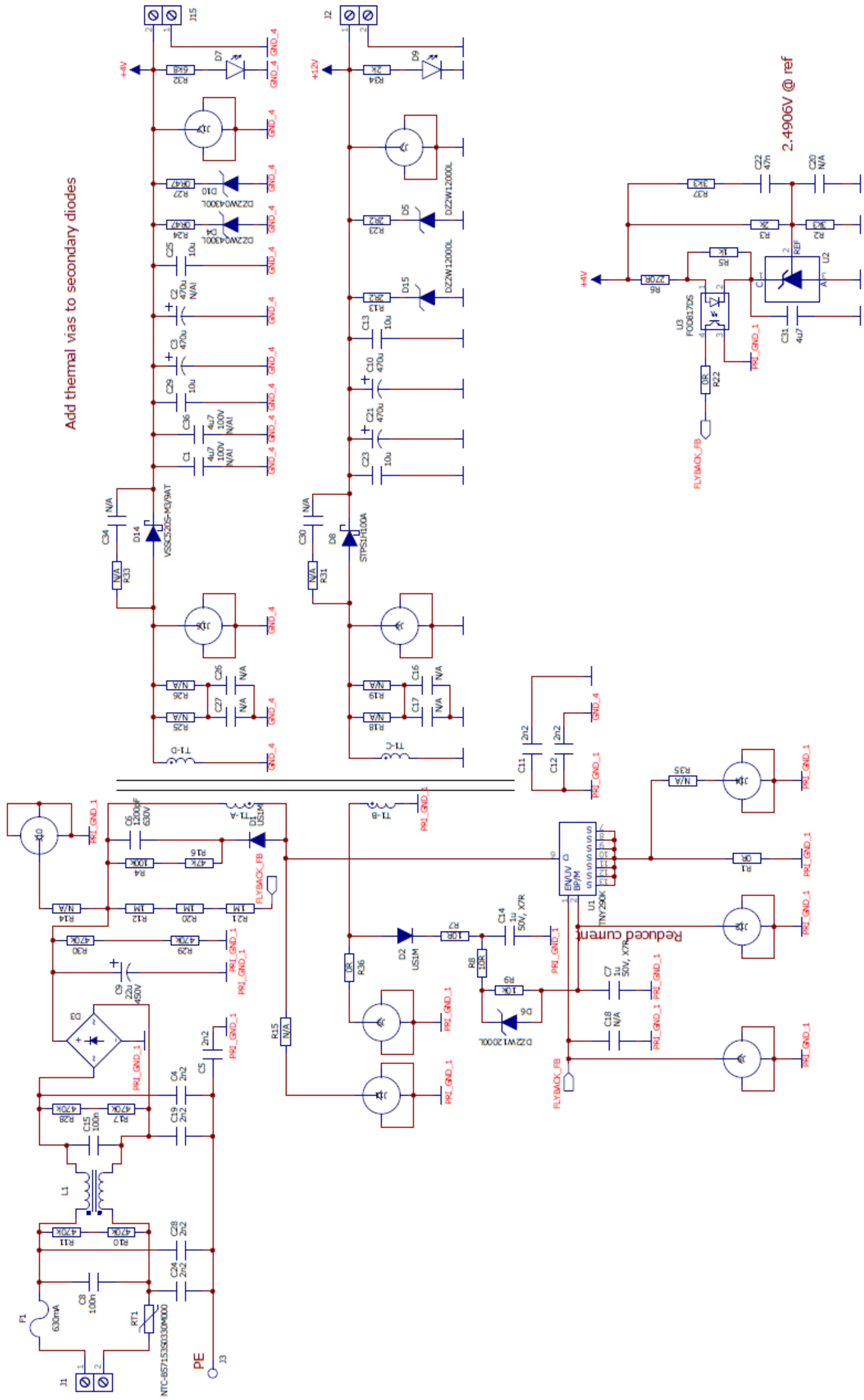

Figure 30. Schematic of second prototype.

The second prototype was based on TNY290K (U1) from Tinyswitch-4 series by Power Integrations. Tinyswitch-4 family has 7 different versions for different power levels (TNY284 to TNY290), so naturally the version with highest power rating was chosen to avoid any further risks of not reaching the output power. SMD package is chosen for automated pick-and-place. According to the datasheet, this model should be capable of up to 20 W output in non-ventilated enclosure, which is suitable for requirement of this thesis [30].

As the typical switching frequency of 132 kHz fits together with the range used for calculating transformer for Altair (top limited to 166 kHz), there was no need to re-calculate the transformer. A lot of the schematic was already developed and could be re-used, e.g. the mains input up to DC-link capacitor (C9) and entire secondary with the addition of optocoupler (U3) for feedback. This was also a good chance to add optional improvements for troubleshooting the power supply that had to be added using prototyping methods which reduced the look of presentability of the device. Such features were additional electrolytic capacitors to secondaries (C2 and C21) and LEDs (D7 and D9) to indicate that the output is powered. By this stage it was also identified that the final product incorporating the power supply needs to be connected to PE (protective earth) which lead to adding surpression capacitors (C4, C19, C24 and C28) between AC input and PE, necessity and values for which shall be determined when conducted emissions are being tested.

Although the protective zeners remained available as component pads, they were not assembled. This type of voltage clamping, although protective, is highly wasteful and shall be used only as a last resort.

Similar to the previous prototype, most of the schematic followed reference design. Additional protection is available due to the auxiliary winding, which allows for sensing failed optocoupler feedback.

The optocoupler, which was not used on previous prototype, requires looking into the frequency characteristic to provide stable output with all sorts of loads and avoid it from oscillating. TL431 programmable reference (U2) can be considered a voltage-controlled NPN-transistor, conducting when reference pin has higher voltage applied than the reference voltage for the shunt device (typically 2.5 V). The voltage divider calculation is not worth explaining in detail. It should be pointed out that TL431 requires specific load capacitance between cathode and anode to avoid oscillations. This can be overlooked easily, as proven by the lacking of which was found after PCBs had been ordered. Values below 6 nF and above 3 μF are suitable for all models of TL431. Attempts to keep the load below 6 nF may be foiled due to parasitics, therefore using 4.7 μF capacitor appears to cover the requirements reliably.

Values for resistors in series ($R_{oc\text{-}ser}$ or R6 on schematic) and parallel ($R_{oc\text{-}par}$ or R5 on schematic) with the optocoupler are derived and verified according to the controller-side. The EN/UV pin is pulled high to DC input through megaohm-range resistors. Optocoupler needs to be capable of sinking this current. Megaohm-range resistors (R12, R20, R21) are chosen according to the desired input voltage for undervoltage-lockout function. Controller starts up as soon as EN/UV pin has 25 μA available for sinking. As universal input for mains is often considered 85 to 265 VAC by major manufacturers (e.g. TI [31]), setting the lockout voltage to 75 VAC (or ~106 VDC) should give enough room for error. Calculation for resistor value without taking the maximum voltage of 2.8 V on EN/UV pin into account gives result of 4.24 MΩ. It is reasonable to combine 3 resistors from E24 series with values of 1.30, 1.30 and 1.60 MΩ, resulting in 4.20 MΩ which is fairly close to calculated value (resulting in 105 VDC or ~74.4 VAC for lockout voltage).

The maximum current expected at 265 VAC (373.65 VDC) is ~89 μA. This is the current optocoupler needs to be capable of sinking.

The initial choice for optocoupler (U3) was FOD817DS, which has transfer ratio between 300 to 600 %. With the minimal transfer ratio of 300 %, minimal optocoupler LED current is found as follows:

$$I_{LED} \geqslant CTR \cdot I_{EN/UV} = \frac{300}{100} \cdot 89 \cdot 10^{-6} = 29.67 \mu A \tag{40}$$

Compared to emitter's maximum forward current of 50 mA, the value of 29.67 μA is extremely low and can be increased for reliability. The power input being 4 V and forward voltage-drop of 0.8 to 1.3V on LED, voltage-drop needs to be taken into account. Target LED current shall be 10 mA, for which the average voltage-drop is 1.2 V.

$$R_{opto} = \frac{V_{in} - V_{f(opto)}}{I_{LED}} = \frac{4 - 1.2}{10 \cdot 10^{-3}} = 280 (ohm) \tag{41}$$

With the value not too critical, the closest match of 270 Ω from E24 series is chosen.

To guarantee the minimum recommended cathode current of 1 mA for TL431 while the LED voltage-drop has not been reached and it is not conducting, additional resistor is applied in series with optocoupler. This is calculated using 1 mA and 1.2 V forward voltage. 1.2 kΩ being the ideal value, 1 kΩ is deemed suitable.

12.1 Various tests

Replacement of the controller went smoother than expected. After powering up the new prototype, no issues occurred - maximum specified load was reached without any issues when using both 115 VAC and 230 VAC input.

Tests used N87 core material unless specified otherwise, as this is the primary candidate availability and price-wise.Output power

After recording the nominal power output, maximum output before protection stopping the controller was recorded.

Table 10. Maximum output power.

Input voltage [VAC]	Output at 4 V [V / A / W]	Output at 12 V [V / A / W]	Total output [W]
115	4.09 / 1.00 / 4.09	14.50 / 0.81 / 11.69	15.78
230	4.09 / 1.00 / 4.09	14.40 / 0.91 / 13.10	17.19

12.1.1 Efficiency

Efficiency was measured using Voltech's PM300 for input power metering and taking readings with various loads.

Table 11. Efficiency results.

115 VAC				
4 V rail load [W]	12 V rail load [W]	Total output load [W]	Input consumption [W]	Efficiency [%]
0	0	0	0.26	0.00
1	0	1	1.82	54.95
4	0	4	5.97	67.00
4	5	9	12.90	69.77

230 VAC				
4 V rail load [W]	12 V rail load [W]	Total output load [W]	Input consumption [W]	Efficiency [%]
0	0	0	0.58	0.00
1	0	1	1.98	50.51
4	0	4	6.46	61.92
4	5	9	13.26	67.87

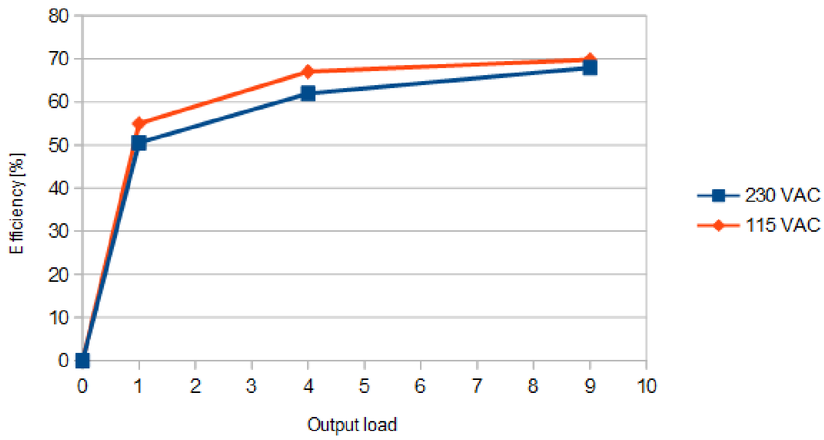

Figure 31. Efficiency results.

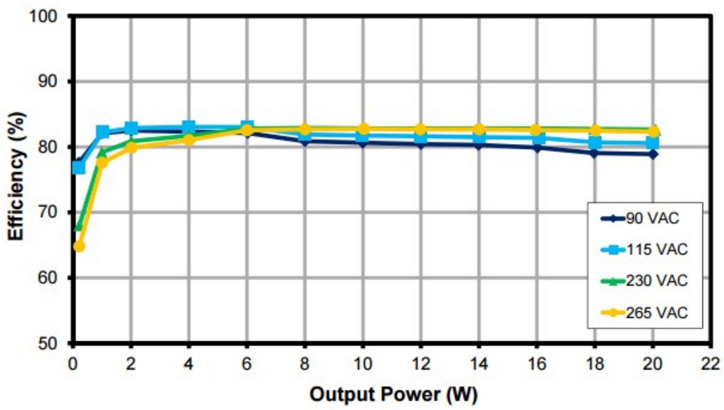

Figure 32. Efficiency of reference design.

Results acquired are slightly below the performance described by reference design, however completely acceptable [32].

12.1.2 Ferrite types

The primary goal for this test is to verify which cores are suitable for nominal output load. Efficiency was not of interest. Transformer bobbin (including the windings) remained the same, only cores were changed.

Load on 4 V rail was kept constant (1 A) and increased on 12 V rail until power supply stopped operating.

Table 12. Maximum load with various core materials.

		N87	3F3	PL-7
230	4V V	4.09	4.09	4.09
	4V I	1.00	1.00	1.00
	4V P	4.09	4.09	4.09
	12 V V	14.40	14.50	14.40
	12 V I	0.91	0.88	0.87
	12V P	13.10	12.82	12.54
	Total W	**17.19**	**16.91**	**16.63**
115	4V V	4.09	4.09	4.09
	4V I	1.00	1.00	1.00
	4V P	4.09	4.09	4.09
	12 V V	14.50	14.50	14.40
	12 V I	0.81	0.78	0.78
	12V P	11.69	11.31	11.23
	Total W	**15.78**	**15.40**	**15.32**

Test shows that all core material candidates are suitable for this application.

12.2 Noise

Although initially planned, the measurement equipment (spectrum analyzer and LISN) for conducted emissions pre-compliance testing was not available during the time window between prototype wake-up and presentation of the thesis.

12.2.1 Output noise

Output noise is measured only with N87 core material. Cases of no load and nominal load are covered for 115 VAC and 230 VAC input voltages.

115 VAC

No load

Nominal load

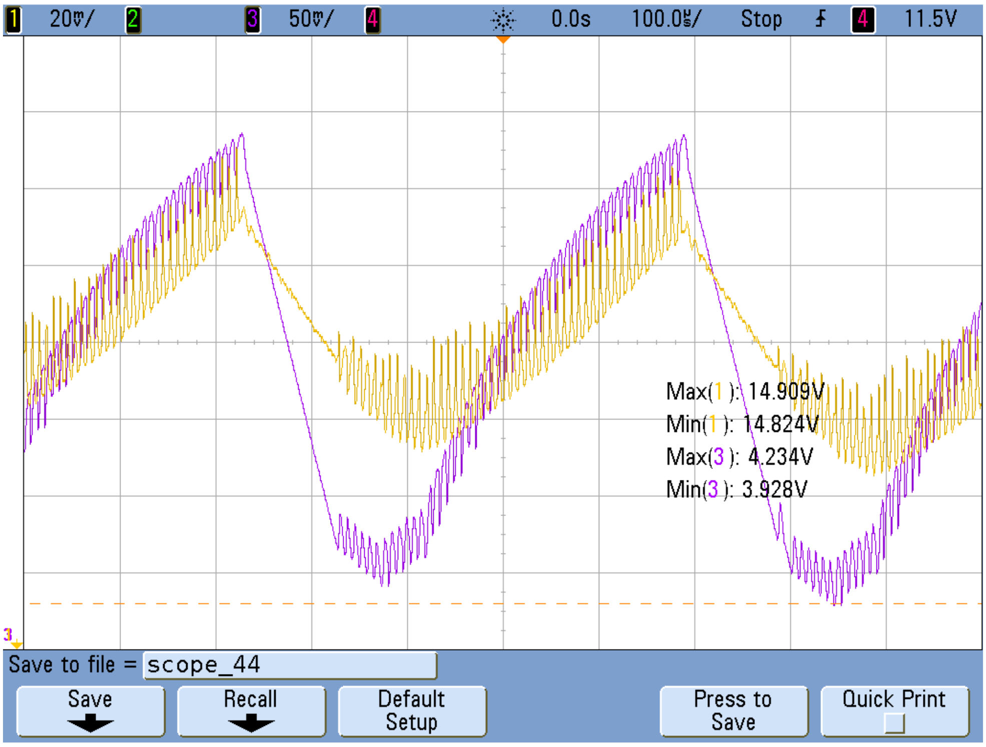

Figure 33. Output ripples at 115 VAC input voltage.

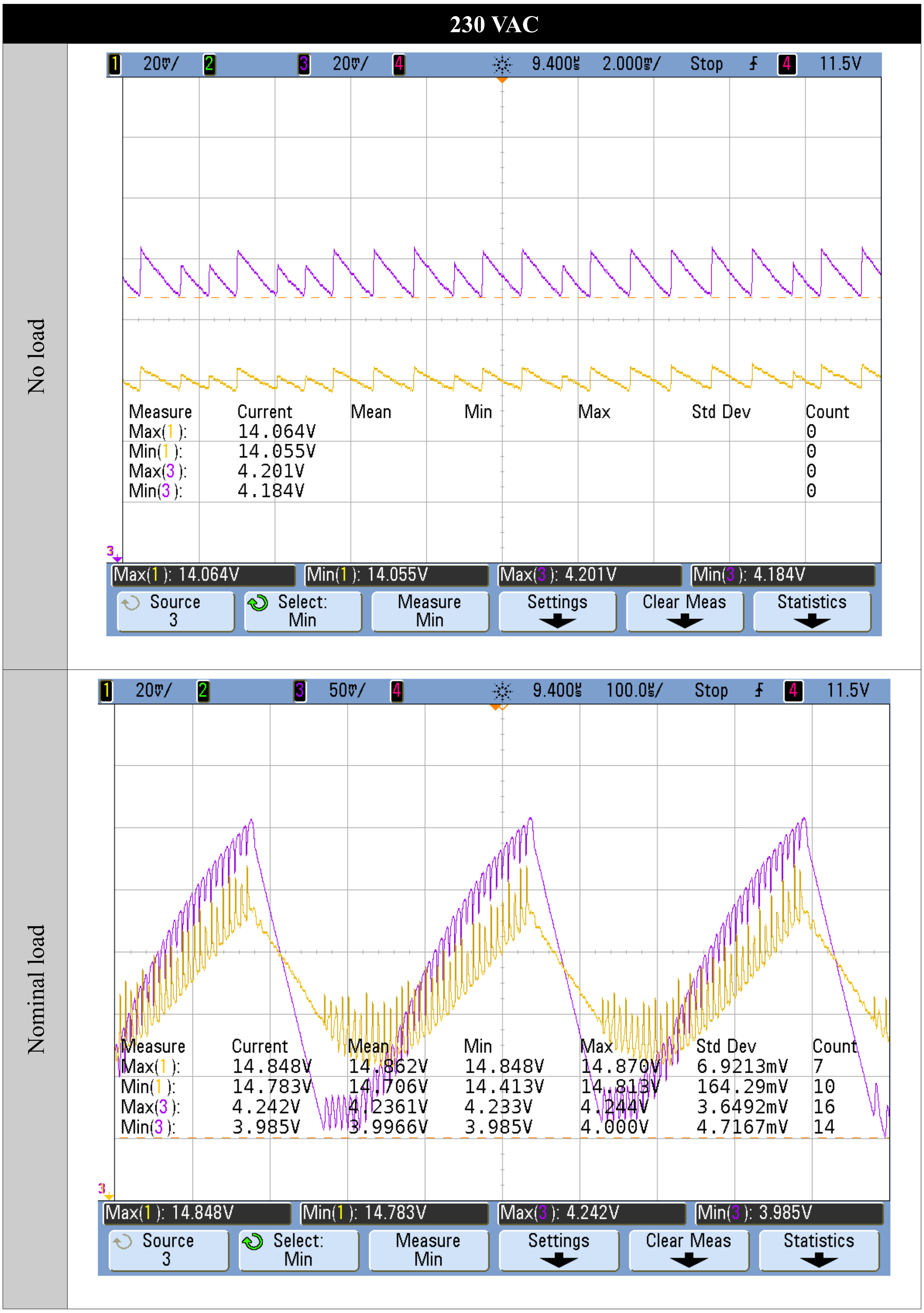

Figure 34. Output ripples at 230 VAC input voltage.

Output noise is fairly identical for both input voltage ranges. From load images it might seem that ripple response for 4 V output could be improved by adjusting the compensation values. Currently it appears that the controller is perfoming switching slightly longer than necessary (starts switching when voltage drops to roughly 3.92 V and stops 4.23 V), but this appears to be more complex, as no-load image shows that switching starts at 4.18 V instead of previously mentioned 3.92 V. Current result is suitable input for the following supply generating 3.3 V and therefore this is considered optional improvement.

12.3 Power factor

Power factor was measured using Voltech's PM300, output load being the nominal load (1 A on 4 V rail and 0.4 A on 12 V rail).

Table 13. Power factor results.

Input voltage	Power factor
115 VAC	0.673
230 VAC	0.679

Resulting values match with values provided in literature, stating that for power supplies using diode-bridge and capacitor in input the power factor is typically 0.6 to 0.7 [28].

Figure 35. Input voltage and current waveform - 115 VAC.

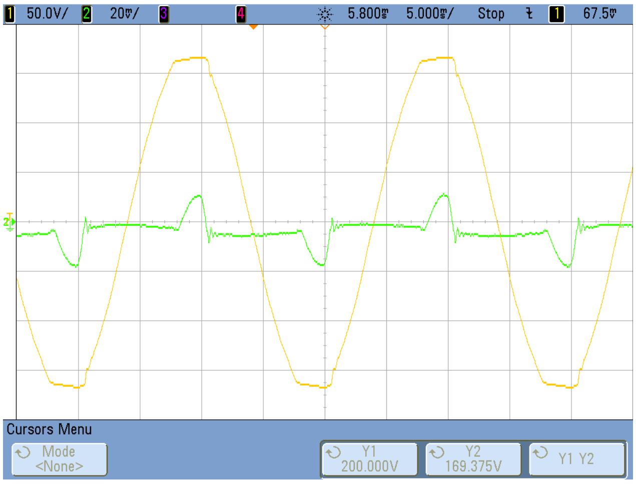

Figure 36. Input voltage and current waveform - 230 VAC.

For illustrative purposes, current and voltage waveforms were recorded, seen in Figure 35 and Figure 36. Due to limited measuring capability, the amplitude values are invalid, however waveform shapes are valid.

12.4 Inrush

Inrush measurement was performed using 0.1 Ω shunt with 1 % tolerance monitored with oscilloscope. To simulate absolute worst-case scenario (plugging in during sine-wave peak), capacitor bank of 12 x 120 µF (resulting in 1440 µF) was charged to 330 VDC (continuously during test) and connected to power supply input.

Voltage peak of 888 mV translates to peak current of 8.79 to 8.97 A (taking into account the shunt tolerance).

Figure 37. Inrush measurement.

12.5 Undervoltage and overvoltage

Input for power supply was provided through autotransformer and output of the autotransformer monitored with a digital multimeter (Kyoritsu KEW 1011).

Tests performed with nominal load (1 A on 4 V rail and 0.4 A on 12 V rail).

While reducing the input voltage down to 66 VAC no changes in behaviour were detected. Continuing to reduce the voltage showed erratic behaviour where controller seemed to be partially restarting with completely shutting down at 61 VAC.

This value of 66 VAC differs from calculated 74 VAC, but is acceptable.

Overvoltage was not tested further than only the maximum rated operating voltage of 265 VAC. No differences were detected when comparing to regular behaviour.

12.6 Operation temperature

Measurement of operation temperature was performed after running the power supply with nominal load (1 A on 4 V rail and 0.4 A on 12 V rail) for 20 minutes to allow temperature to stabilize. For each measurement category the point with highest temperature was recorded. Environment temperature remained 27°C throughout the entire test. No means of forced convection (e.g. fans) was used and test was done in still air. Thermometer used was PockeTherm 32.

Table 14. Temperature measurement results.

	115 VAC	230 VAC
Transformer coil	50	54
Transformer core	46	48
Controller	48	59

Maximum temperature rise of 32°C in free air is acceptable, however might need re-testing when casing for final product is clarified. It should be noted that the nominal load for this power supply is specified with margin even in the worst-case estimated consumption for final product.

13 Safety aspects

The final product including the power supply needs to conform to the family standard EN 60730-1:2016, therefore all the limits are specified according to this (and other standards that are referred to by EN 60730-1).

13.1 Creepages and clearances

Working with mains voltage, which stands remarkably higher than any voltages consumers may come in contact with (e.g. batteries or phone chargers) poses risks like arcing. To guarantee electrical safety, rules have been collected and presented as standards.

The necessary gaps determined to be reasonably safe are divided into two categories - creepages and clearances. Clearance being direct line-of-sight distance between two points, where no pollution (e.g. dust) cannot accumulate and creepage being the opposite, meaning distance needed to travel across surface. Adding clearance distance is more difficult as it needs constructing an obstruction between two points, however creepage can be increased easily by routing an air gap in PCB between the two offending points [33]. Examples of creepage and clearance are provided in Figure 38.

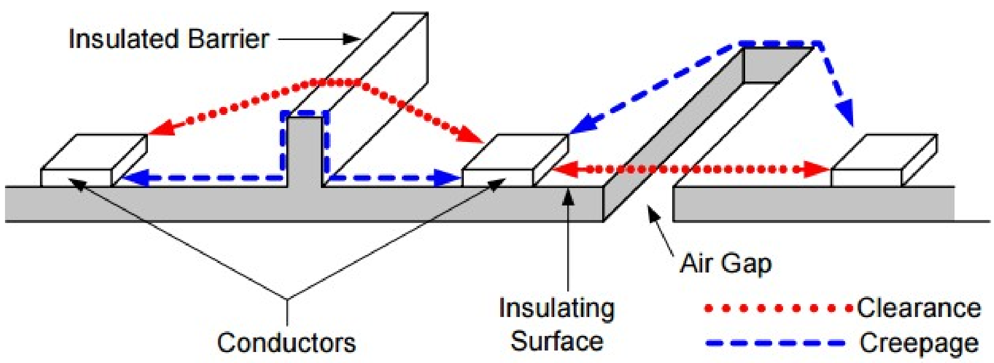

Figure 38. Creepage and clearance visualised.

Only primary side is covered in this chapter, as secondary side is rated below 50 V (classifies as ELV circuit) and applicable clearances (< 0.20 mm) are guaranteed by PCB design rules. Safety creepage/clearance-wise is not as critical for secondary.

The device is designed for pollution degree II as most suitable for household environment.

Applying transient-voltage surpressor to mains input on power supply (not done on prototypes) shall allow using overvoltage category II, instead of overvoltage category III.

For PCB the material group is specified to be IIIa (CTI from 175 up to 400) or better. This appears to be minimum that PCB manufacturers specify [34]. If this is not specified (and PCB manufacturer can/will not specify it), this PCB should not be used for this application, as material group IIIb is not permitted for applications using voltages above 630 V (which can occur in this application).

Double insulation, which recedes to literally double the gap size due to definitions of basic and supplementary insulation in EN 60730-1:2016, shall be guaranteed between primary and secondary. Anywhere else only functional isolation is required.

The first step is to map out the voltages (RMS) between various points. All values are rounded up to closest value of creepage distance table in standard.

Table 15. Power supply voltage map.

	PE	**Mains L/N**	**Switcher drain**	**Rect. mains**
Secondaries	50	400	500	400
PE	-	400	500	400
Mains L/N	400	400	800	800
Switcher drain	500	800	-	500
Rectified mains	400	800	400	400

From mains input to TVS clearance of 0.5 mm or better shall be kept to match corresponding overvoltage class requirements. Operational insulation follows actual RMS values and shall be kept to minimum of 0.2 mm with the exceptions of nets with 800 V difference (only value above 500 V), where clearance of 0.5 mm is used. Clearance of 1.0 mm (double of 0.5 mm) shall be used between primary and secondary.

Following the RMS voltage cross-referencing table, suitable outer layer creepages can be defined.

Table 16. Outer layer creepages, in mm.

	PE	Mains L/N	Switcher drain	Rect. mains
Secondaries	2x 1.2	2x 4.0	2x 5.0	2x 4.0
PE	-	4.0	5.0	4.0
Mains L/N	4.0	4.0	8.0	8.0
Switcher drain	5.0	8.0	-	5.0
Rectified mains	4.0	8.0	4.0	4.0

14 Summary

The task of creating a universal input power supply was solved in multiple iterations after topology selection, starting with a feasibility study. After determining that in large volumes this in fact can reduce the cost of device when compared to an off-the-shelf supply, while also allowing for additional flexibility, development started.

During the development a lot of effort was put into calculating one of the primary components of the chosen topology - the transformer. In parallel with this task the schematic capture was done.

After finishing the design and assembly of the first prototype, testing showed that using the chosen controller caused multiple issues and the goals set for the design may not be achieveable. This led to the second prototype, which was completed successfully, meeting all the requirements that were set earlier.

During the development and testing, attention was paid to adhere to applicable standards regarding electromagnetic emissions and electrical safety.

Sources

[1] G. A. Williamson. (2017, April 22). Power supplies [Online]. Available: http://www.williamson-labs.com/powersupply.htm

[2] No author given. (2017, April 22). High Input Voltage Linear Regulator [Online]. Available: http://www.learningelectronics.net/circuits/high-input-voltage-linear-regulator.html

[3] Texas Instruments. (2017, April 22). Texas Instruments Power Topologies [Online]. Available: http://www.ti.com/lit/sg/sluw001f/sluw001f.pdf

[4] A. Pressman, K. Billings, et al, Switching power supply design. New York: McGraw-Hill Companies, 2009

[5] Farnell element14. (2017, April 15). XP POWER ECL15UD03-T entry [Online]. Available: http://ee.farnell.com/xp-power/ecl15ud03-t/ac-dc-psu-dual-o-p-15w-chassis/dp/1860898

[6] ST Microelectronics. (2017, April 15). Altair05T-800 datasheet [Online]. Available: http://www.st.com/content/ccc/resource/technical/document/datasheet/f2/10/b8/8e/fd/60/4b/20/CD00285102.pdf/files/CD00285102.pdf/jcr:content/translations/en.CD00285102.pdf

[7] Infineon Technologies AG. (2017, April 15). Quasi-resonant control with XMC1000 [Online]. Available: http://www.infineon.com/dgdl/Infineon-ApplicationNote_Quasi_Resonant_Control_XMC1000-AN-v01_00-EN.pdf?fileId=5546d462557e6e890155a05c4b285c9f

[8] J. Harper. (2017, April 15). What a quasi-resonant converter does for you [Online]. Available: http://www.eetimes.com/document.asp?doc_id=1278790

[9] Voltech Instruments Ltd.. (2017, April 15). Measuring Leakage Inductance [Online]. Available: http://www.voltech.com/Articles/104-105%20Leakage%20Inductance/104-105.pdf

[10] L. Dixon. (2017, April 15). The Effects of Leakage Inductance on Multi-Output Flyback Circuits [Online]. Available: http://www.ti.com/lit/ml/slup081/slup081.pdf

[11] M. Dekker. (2017, April 15). Transformer and Inductor Design Handbook [Online]. Available: http://coefs.uncc.edu/mnoras/files/2013/03/Transformer-and-Inductor-Design-Handbook_Chapter_17.pdf

[12] J. Picard. (2017, April 15). Under the Hood of Flyback SMPS Designs [Online]. Available: http://e2e.ti.com/cfs-file/__key/communityserver-discussions-components-files/188/5635.Under-the-Hood-of-Flyback-SMPS-Designs.pdf

[13] B. Keogh, I. Cohen. (2017, April 15). Flyback transformer designconsiderations for efficiencyand EMI [Online]. Available: https://www.ti.com/seclit/ml/slup338/slup338.pdf

[14] J. Adams. (2017, April 15). Flyback Transformer Design for the IRIS40xx Series [Online]. Available: http://www.infineon.com/dgdl/an-1024.pdf?fileId=5546d462533600a401535591115e0f6d

[15] Ronald Dekker. (2017, April 15). Flyback Converters for Dummies [Online]. Available: http://www.dos4ever.com/flyback/flyback.html

[16] EPCOS AG. (2017, April 15). E 20/10/6 (EF 20)Core and accessories [Online]. Available: https://en.tdk.eu/inf/80/db/fer_13/e_20_10_6.pdf

[17] EPCOS AG. (2017, April 15). EP5 core datasheet [Online]. Available:

https://en.tdk.eu/inf/80/db/fer_13/ep_5.pdf
[18] Vishay. (2017, April 15). Professional Thin Film Chip Resistors datasheet [Online]. Available: http://www.vishay.com/docs/28705/mc_pro.pdf
[19] IET LABS, Inc. (2017, April 15). Skin Effect on Wire [Online]. Available: http://www.ietlabs.com/pdf/application_notes/036003%201900%20Skin%20Effect%20on%20Wire.pdf
[20] F. Cathell. (2017, April 15). Increasing Low PowerConverter Efficiency withResonant Snubbers [Online]. Available: https://www.onsemi.com/pub/Collateral/AND8296-D.PDF
[21] No author given. (2017, April 15). How to design a snubber for a flyback converter [Online]. Available: http://how-to.wikia.com/wiki/How_to_design_a_snubber_for_a_flyback_converter
[22] M. Berman. (2017, April 22). All about EMI filters [Online]. Available: http://www.electronicproducts.com/Passive_Components/Circuit_Protection/All_about_EMI_filters.aspx
[23] KEMET. (2017, April 15). SU Coils, SU 9V/9H Type datasheet [Online]. Available: http://www.farnell.com/datasheets/1760497.pdf
[24] D. Herres. (2017, April 15). How To Measure Power Factor With An Oscilloscope [Online]. Available: http://www.testandmeasurementtips.com/measure-power-factor-oscilloscope/
[25] TDK. (2017, April 15). TDK product C3225X7S1H106K250AB description [Online]. Available: https://product.tdk.com/en/search/capacitor/ceramic/mlcc/info?part_no=C3225X7S1H106K250AB
[26] Taiyo Yuden. (2017, April 15). Capacitor TMK212BBJ106KGHT description [Online]. Available: http://ds.yuden.co.jp/TYCOMPAS/ut/detail.do?productNo=TMK212BBJ106KGHT&dataUnit=M
[27] B. Bose, Power Electronics and Motor Drives. Burlington, MA: Elsevier Inc., 2006
[28] K. Billings, T. Morey, Switchmode Power Supply Handbook. New York: McGraw-Hill Companies, 2011
[29] Fairchild Semiconductor Corporation. (2017, April 15). Design Guideline for Flyback Charger Using FAN104WMX [Online]. Available: https://www.fairchildsemi.com/application-notes/AN/AN-6093.pdf
[30] Power Integrations. (2017, April 15). Tinyswitch-4 family datasheet [Online]. Available: https://ac-dc.power.com/sites/default/files/product-docs/tinyswitch-4_family_datasheet.pdf?download=0
[31] Texas Instruments. (2017, April 15). 85 to 265VAC Input 5V/7.5W Low Cost Small Size Flyback Reference Design [Online]. Available: http://www.ti.com/tool/pmp9045
[32] Power Integrations. (2017, April 15). Reference Design Report for a 20 W StandbyPower Supply Using TinySwitchTM-4TNY290PG [Online]. Available: https://ac-dc.power.com/sites/default/files/PDFFiles/rdr295.pdf
[33] B. Mammano, L. Bahra. (2017, April 15). Safety Considerations in Power Supply Design [Online]. Available: https://www.ieee.li/pdf/essay/safety_considerations_in_power_supply_design.pdf
[34] Bicheng Enterprise Ltd. (2017, April 15). High CTI 600V PCB [Online]. Available: http://www.bicheng-enterprise.com/en/about/High%20CTI%20PCB.asp

Appendix 1 - BOM for first prototype

Qty	Reference	Part Name	Manufacturer	Description	Value	Rating
1	U1	ALTAIR05T-800	STMICROELECTRONICS	Off-line all-primary-sensing switching regulator, SO16		
1	D2	BAS316,115	NXP	Small Signal Diode, Single, 100 V, 250 mA, 1.25 V, 4 ns, 4 A		250mA, 100V
1	C3			SMD 0603 Cap.	1n5	16V
1	C1			SMD 0603 Cap.	4n7	16V
1	C2			SMD 0603 Cap.	680n	16V
2	C4-5			SMD 0603 Cap.	N/A	16V
1	C14			SMD 0603 Cap.	N/A	25V
4	C16-19			SMD 0805 Cap.	N/A	16V, X7R
1	C6	CGA5F4C0G2J122J085AA	TDK	SMD MLCC	1200pF	630V
1	C9	EEUED2W220S	PANASONIC ELECTRONIC COMPONENTS	Electrolytic cap	22u	450V
2	C10-11	UPW1H471MHD1TO	NICHICON	ELECTROLYTIC CAPACITOR, 470UF, 50V, 20%, RADIAL	470u	50V
3	C7 C12-13	C3225X7S1H106K250AB	TDK	MLCC, 10 µF, ± 10%, X7S, 50 V, 1210	10u	50V
2	C8 C15	B32922C3104M000	EPCOS	X2 safety capacitor	0.1u	305VAC
1	L1	SU9V-07010	KEMET	Common mode choke	1m	700mA
3	J1-3	MKDSN2,5/2-5.08	PHOENIX CONTACT	Screw terminal, 2pos, 5.08mm		16A, 400V
9	J4-12	73412-0110	Molex	SMD Coax con. Receptacle 50Ohm	n/a	
1	D4	DZ2W04300L	PANASONIC ELECTRONIC COMPONENTS	Zener, 4.3V, 1W, SOD-123F	4V3	1W, 200mA
1	D5	DZ2W13000L	PANASONIC ELECTRONIC COMPONENTS	Zener, 13V, 1W, SOD-123F	13V	1W, 200mA
1	D8	STPS1H100A	STMICROELECTRONICS	Schottky, 100 V, 1 A, 620 mV, 50 A		Vrrm=100V, Ifavg=1A
1	D3	DBLS107G	Multicomp	Bridge Rectifier, 1 kV, 1 A		Ifavg=1A, Vrrm=1kV
1	F1	MCMET 630MA 250V	MULTICOMP	Fuse, 0.63A, slow blow, 250VAC	630mA	
4	X1-4			NOT ASSEMBLED!	n/a	
1	RT1	B57153S0330M000	EPCOS	NTC, 33R @ Imin, 0.832R @ Imax	33R	1.3A
1	D7	PMEG3015EJ,115	NXP	Ultra low VF Schottky barrier rectifiers		Ifavg=1.5A, Ipk=9A, Ufmax=550mV
1	R3			RES 0603	0R	0W1
1	R9			RES 0603	10R	0W1
1	R7			RES 0603	13k	0W1
1	R5			RES 0603	150R	0W1
1	R2			RES 0603	15k	0W1
1	R6			RES 0603	2k7	0W1
1	R8			RES 0603	470R	0W1
1	R12			RES 0805	0R47	0W125
1	R4			RES 0805	100k	0W125
1	R13			RES 0805	2R2	0W125
1	R16			RES 0805	47k	0W125
4	R18-21			RES 0805	N/A	0W125
1	R1	ERJ1TYJ1R0U ERJ1TYJ1R0U	PANASONIC ELECTRONIC COMPONENTS	SMD Resistor 2512	1R	1W
3	R10-11 R17			CARBON FILM RESISTOR	1M	2W
2	R14-15			Jumper - Proto only	N/A	2W
1	T1			Flyback transformer, designed for 85-250VAC in, 12VDC & 4VDC out		
1	D1	US1M	Multicomp	Ultrafast Power Diode, Single, 1 kV, 1 A, 1.7 V, 75 ns, 30 A		700V RMS, 1A

Appendix 2 - BOM for second prototype

Qty	Reference	Part Name	Manufacturer	Description	Value	Rating
1	U2	KA431SMFTF	Fairchild	Programmable shunt reference	2.5V	
1	C22			SMD 0603 Cap.	47n	16V
2	C18 C20			SMD 0603 Cap.	N/A	16V
2	C7 C14	GRM21BR71H105KA12L	MURATA	SMD 0805 Cap.	1u	50V, X7R
1	C31	GRM21BR71H105KA12L	MURATA	SMD 0805 Cap.	4u7	50V, X7R
4	C16-17 C26-27			SMD 0805 Cap.	N/A	16V, X7R
1	C30			SMD 0805 Cap.	N/A	50V, X7R
1	C34			SMD 0805 Cap.	N/A	63V, X7R
1	C6	CGA5F4C0G2J122J085AA	TDK	SMD MLCC	1200pF	630V
1	C9	EEUED2W220S	PANASONIC ELECTRONIC COMPONENTS	Electrolytic cap	22u	450V
4	C2-3 C10 C21	UPW1H471MHD1TO	NICHICON	ELECTROLYTIC CAPACITOR, 470UF, 50V, 20%, RADIAL	470u	50V
4	C13 C23 C25 C29	C3225X7S1H106K250AB	TDK	MLCC, 10 µF, ± 10%, X7S, 50 V, 1210	10u	50V
2	C1 C36	C4532X7S2A475M230KB	TDK	Cap, MLCC, 1812	4u7	100V
2	C8 C15	B32922C3104M000	EPCOS	X2 safety capacitor	100n	305VAC
7	C4-5 C11-12 C19 C24 C28	B32021A3222M000	TDK	EMI Suppression Capacitor, 2.2NF, 300V, 10mm pin spacing	2n2	300V
1	L1	SU9V-07010	KEMET	Common mode choke	1m	700mA
3	J1-2 J15	MKDSN2,5/2-5.08	PHOENIX CONTACT	Screw terminal, 2pos, 5.08mm		16A, 400V
10	J4 J7-12 J14 J16-17	73412-0110	Molex	SMD Coax con. Receptacle 50Ohm	n/a	
2	D4 D10	DZ2W04300L	PANASONIC ELECTRONIC COMPONENTS	Zener, 4.3V, 1W, SOD-123F	4V3	1W, 200mA
3	D5-6 D15	DZ2W12000L	PANASONIC ELECTRONIC COMPONENTS	Zener, 12V, 1W, SOD-123F	12V	1W, 200mA
1	D8	STPS1H100A	STMICROELECTRONICS	Schottky, 100 V, 1 A, 620 mV, 50 A		Vrrm=100V, Ifavg=1A
1	D14	VSSC520S-M3/9AT	VISHAY SEMICONDUCTOR	Schottky, Single, 200 V, 5 A, 1.7 V, 100 A, 150 °C		5A, 200V
1	D3	DBLS107G	Multicomp	Bridge Rectifier, 1 kV, 1 A		Ifavg=1A, Vrrm=1kV
1	U3	FOD817DS	Fairchild Semiconductor	OPTOISOLATOR		5 kV rms
1	F1	MCMET 630MA 250V	MULTICOMP	Fuse, 0.63A, slow blow, 250VAC	630mA	
2	D7 D9	OVS-0801	MULTICOMP	LED 0805 White		
4	X1-4			NOT ASSEMBLED!	n/a	
1	RT1	B57153S0330M000	EPCOS	NTC, 33R @ Imin, 0.832R @ Imax	33R	1.3A
1	R22			RES 0603	0R	0W1
2	R7-8			RES 0603	10R	0W1
1	R9			RES 0603	10k	0W1
1	R5			RES 0603	1k	0W1
1	R6			RES 0603	270R	0W1
2	R3 R34			RES 0603	2k	0W1
2	R2 R37			RES 0603	3k3	0W1
1	R32			RES 0603	6k8	0W1
2	R24 R27			RES 0805	0R47	0W125
1	R4			RES 0805	100k	0W125
2	R13 R23			RES 0805	2R2	0W125
1	R16			RES 0805	47k	0W125
6	R18-19 R25-26 R31 R33			RES 0805	N/A	0W125
6	R10-11 R17 R28-30			RES 1206	470k	0W25
1	R1	ERJ1TYJ1R0UERJ1TYJ1R0U	PANASONIC ELECTRONIC COMPONENTS	SMD Resistor 2512	0R	1W
1	R36	ERJ8ENF1204V	PANASONIC ELECTRONIC COMPONENTS	SMD Resistor 1206	0R	250mW
3	R12 R20-21	ERJ8ENF1204V	PANASONIC ELECTRONIC COMPONENTS	SMD Resistor 1206	1M	250mW
3	R14-15 R35	ERJ8ENF1204V	PANASONIC ELECTRONIC COMPONENTS	SMD Resistor 1206	N/A	250mW
1	J3			1.2mm(diam) hole with 1.6mm(diam) pad		
1	U1	TNY290KG	POWER INTEGRATIONS	Off-line switcher		725Vdss, up to 28.5W open frame
1	T1			SMPS transformer		
2	D1-2	US1M	Multicomp	Ultrafast Power Diode, Single, 1 kV, 1 A, 1.7 V, 75 ns, 30 A		700V RMS, 1A